Coordination corrected *ab initio* formation enthalpies
Supplementary Information

Rico Friedrich,[1,2] Demet Usanmaz,[1,2] Corey Oses,[1,2] Andrew Supka,[3] Marco Fornari,[2,3]
Marco Buongiorno Nardelli,[2,4] Cormac Toher,[1,2] and Stefano Curtarolo[2,5,6,*]

[1] *Department of Mechanical Engineering and Materials Science, Duke University, Durham, North Carolina 27708, USA*
[2] *Center for Materials Genomics, Duke University, Durham, North Carolina 27708, United States*
[3] *Department of Physics and Science of Advanced Materials Program, Central Michigan University, Mount Pleasant, Michigan 48859, USA*
[4] *Department of Physics and Department of Chemistry, University of North Texas, Denton, TX 76203, USA*
[5] *Materials Science, Electrical Engineering, Physics and Chemistry, Duke University, Durham NC, 27708, USA*
[6] *Fritz-Haber-Institut der Max-Planck-Gesellschaft, 14195 Berlin-Dahlem, Germany*

(Dated: April 26, 2019)

I. Comparing experimental enthalpy differences with calculated energy differences

In Figure 1(a) the calculated internal energy differences from AGL are plotted *vs.* the experimental enthalpy differences [1] between 0 K and T_r for 52 (36 binary and 16 ternary) oxides. The calculated values approximate the measured data in general very well, with a slight tendency to underestimate them. The MAE is 4, 5 and 5 meV/atom for calculations using PBE, LDA and SCAN, respectively. There are three cases with major deviations: NaO_2, KO_2 and CoO. The largest difference between calculated and experimental values occurs for NaO_2: 30 meV/atom for LDA. Superoxides might be difficult to describe within the AGL Debye model. For CoO the deviation of 15-20 meV/atom can be assigned to the general difficulty of describing the properties of the material as noted before for the calculated formation enthalpy in Fig. 2 in the main text, also recognized previously [2].

In Figure 1(b) an equivalent plot is presented for 29 mostly metallic elements. The MAE is 8, 10 and 9 meV/atom for PBE, LDA and SCAN. In general, the calculations slightly underestimate the experimental enthalpy difference. This can be understood as the AGL approach neglects electronic contributions to the internal energy change. The errors are significantly smaller than the MAEs of CCE in Fig. 3 in the main text, which are of the order of 30 meV/atom.

The combined effect of the thermal excitations for the compounds and elements on the formation enthalpy is illustrated in Fig. 1(c). It depicts the difference $(\Delta_\mathrm{f}H^{\circ,T_\mathrm{r},\mathrm{cal}} - \Delta_\mathrm{f}H^{\circ,0\mathrm{K},\mathrm{cal}})$ *vs.* $(\Delta_\mathrm{f}H^{\circ,T_\mathrm{r},\mathrm{NJ}} - \Delta_\mathrm{f}H^{\circ,0\mathrm{K},\mathrm{NJ}})$ for the same set of compounds as in Fig. 1(a). The MAEs are 3, 4 and 4 meV/atom for PBE, LDA and SCAN, indicating that the underestimation of individual enthalpy differences in Figs. 1(a,b) is partially canceled in the formation enthalpy. The three systems showing large deviations (up to 26 meV/atom for NaO_2) are the same as in Fig. 1(a): the only compounds with a positive experimental difference between 0 K and T_r. In conclusion, the AGL approach treats thermal contributions reliably at low computational cost.

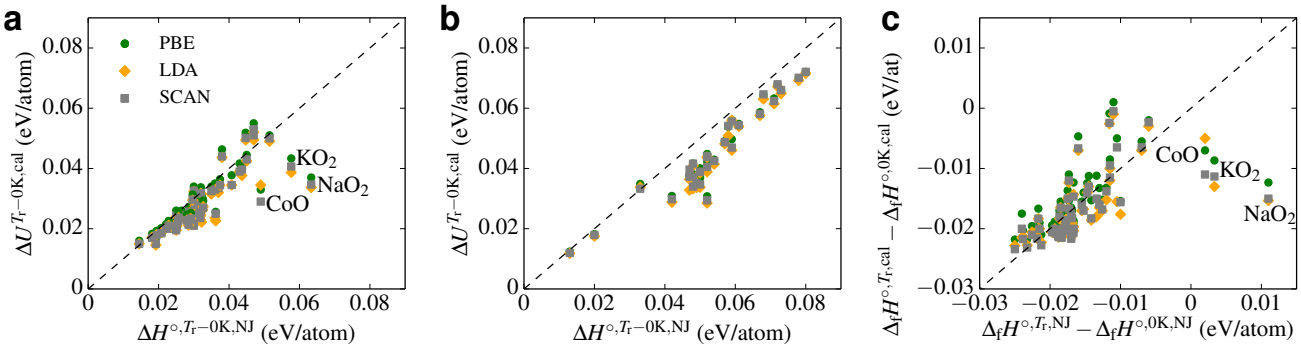

FIG. 1. **Internal energy *vs.* enthalpy differences.** Calculated internal energy differences *vs.* experimental enthalpy differences from the NIST-JANAF (NJ) collection [1] between 0 and T_r=298.15 K for (**a**) binary and ternary oxides and (**b**) elemental reference phases. A comparison of the calculated *vs.* experimental formation enthalpy differences for the same set of compounds as in (**a**) is presented in (**c**). Points showing significant deviations are labeled with the compound in (**a**,**c**).

* stefano@duke.edu

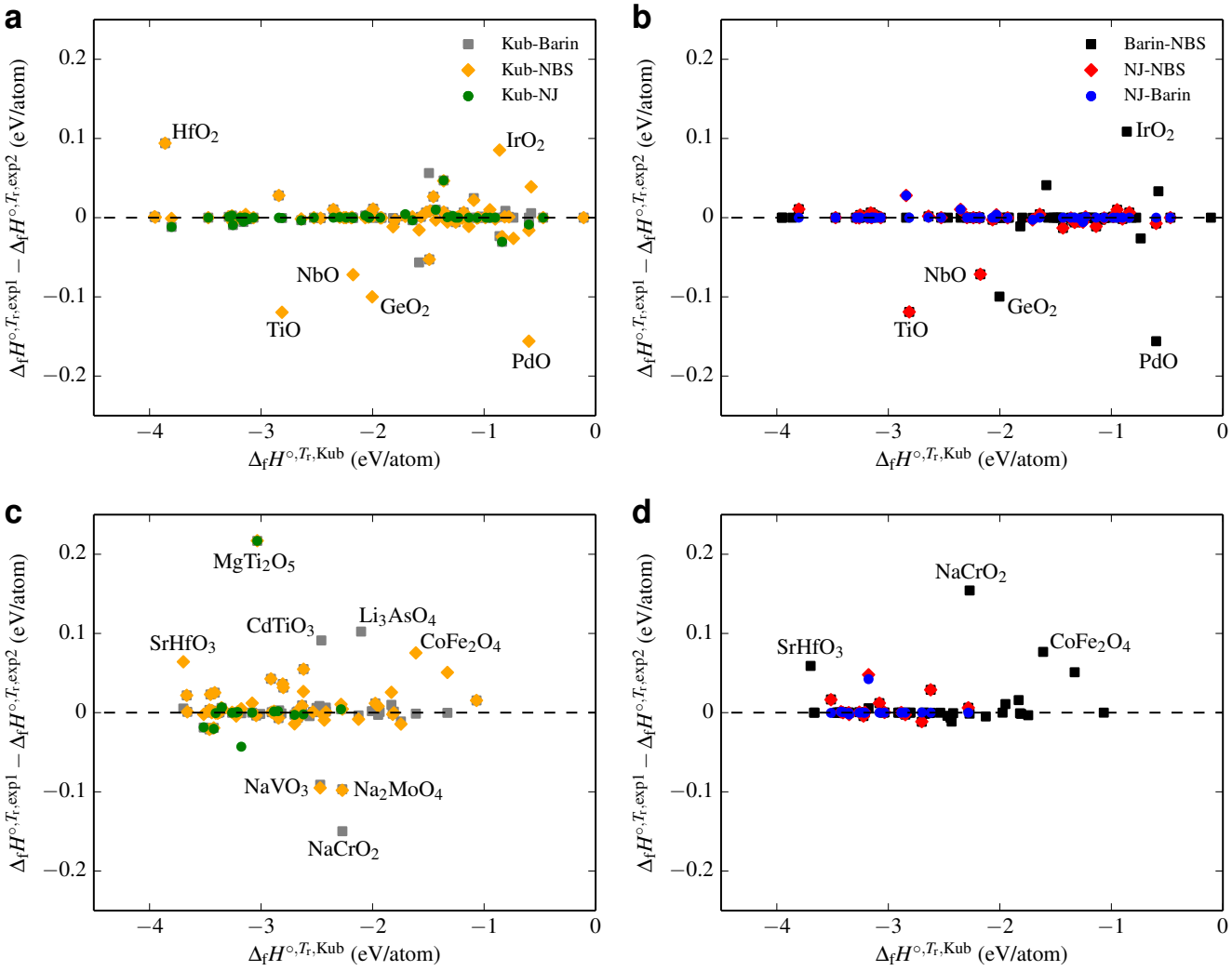

FIG. 2. **Comparison of experimental values.** Comparison of the experimental room temperature formation enthalpies from different sources for binary (**a**,**b**) as well as ternary (**c**,**d**) oxides. Points showing deviations $\gg \pm 50$ meV/atom are labeled with the compound. Kub refers to Ref. [3], NJ to Ref. [1], Barin to Ref. [4] and NBS to Ref. [5]. Despite corrections can be done to bring MAE to 20-50 meV/atom, there is substantial scatter in experimental measurements.

II. Comparing experimental formation enthalpies from different sources

Comparing the data from different experimental sources gives insight on the exact formation enthalpy. Figure 2 shows the difference between the four collections [1, 3–5] for binary (Figs. 2(a,b)) and ternary (Figs. 2(c,d)) oxides. Table I includes the mean absolute deviations. Not all oxides are available in all collections. The number of compounds reported is therefore added in brackets after the name of the collection.

In general, most of the values for one oxide agree well. However, in certain cases, deviations significantly exceeding ± 50 meV/atom are observed, for which the respective compound is labeled. For the binary oxides in Figs. 2(a,b), significant deviations always occur when data from the NBS tables are compared to another source as also indicated by the mean absolute deviations in Table I. The

TABLE I. **Comparison of experimental values.** Mean absolute deviations for the experimental formation enthalpies from different sources for binary (above the diagonal) and ternary (below the diagonal) oxides: Kub (Kubaschewski) [3], NJ [1], Barin [4] and NBS [5]. The numbers in brackets after the abbreviations, in the first row for binary and in the first column for ternary oxides, denote the number of oxides for which formation enthalpies were available. The numbers in brackets in the second column are the mean absolute deviation when $MgTi_2O_5$ is excluded from the set. All values in meV/atom.

	Kub (79)	NJ (41)	Barin (79)	NBS (76)
Kub (71)	-	4	8	14
NJ (16)	20 (7)	-	1	8
Barin (71)	17 (14)	3	-	10
NBS (59)	19 (15)	8	8	-

largest values of 14, 10 and 8 meV/atom are found between NBS and the other collections. This might be due to the special internal consistency requirements inside the NBS tables [5].

For ternary oxides significant deviations are seen between Kubaschewski *et al.* and Barin as well as between Kubaschewski *et al.* and NBS in Fig. 2(c). Some of the formation enthalpies for ternary oxides might not be very accurate in Kubaschewski. For $MgTi_2O_5$, Kubaschewski $\Delta_f H^{\circ,T_r,\mathrm{exp}}$ is clearly inaccurate since all three other collections suggest the same value, which deviates by more than 200 meV/atom. It is a bias to the mean absolute deviation, especially when compared to NIST-JANAF (NJ) as there are only 16 common ternary oxides within the two collections. Therefore, in the second column in Table I the numbers in brackets were calculated with $MgTi_2O_5$ excluded. The largest mean absolute deviations are observed when NBS is involved with the exception of the comparison between Barin and Kubaschewski. In Figure 2(d) three significant deviations are also found between the Barin and NBS collections. Therefore, the NBS data might not be suited for comparisons with calculated results.

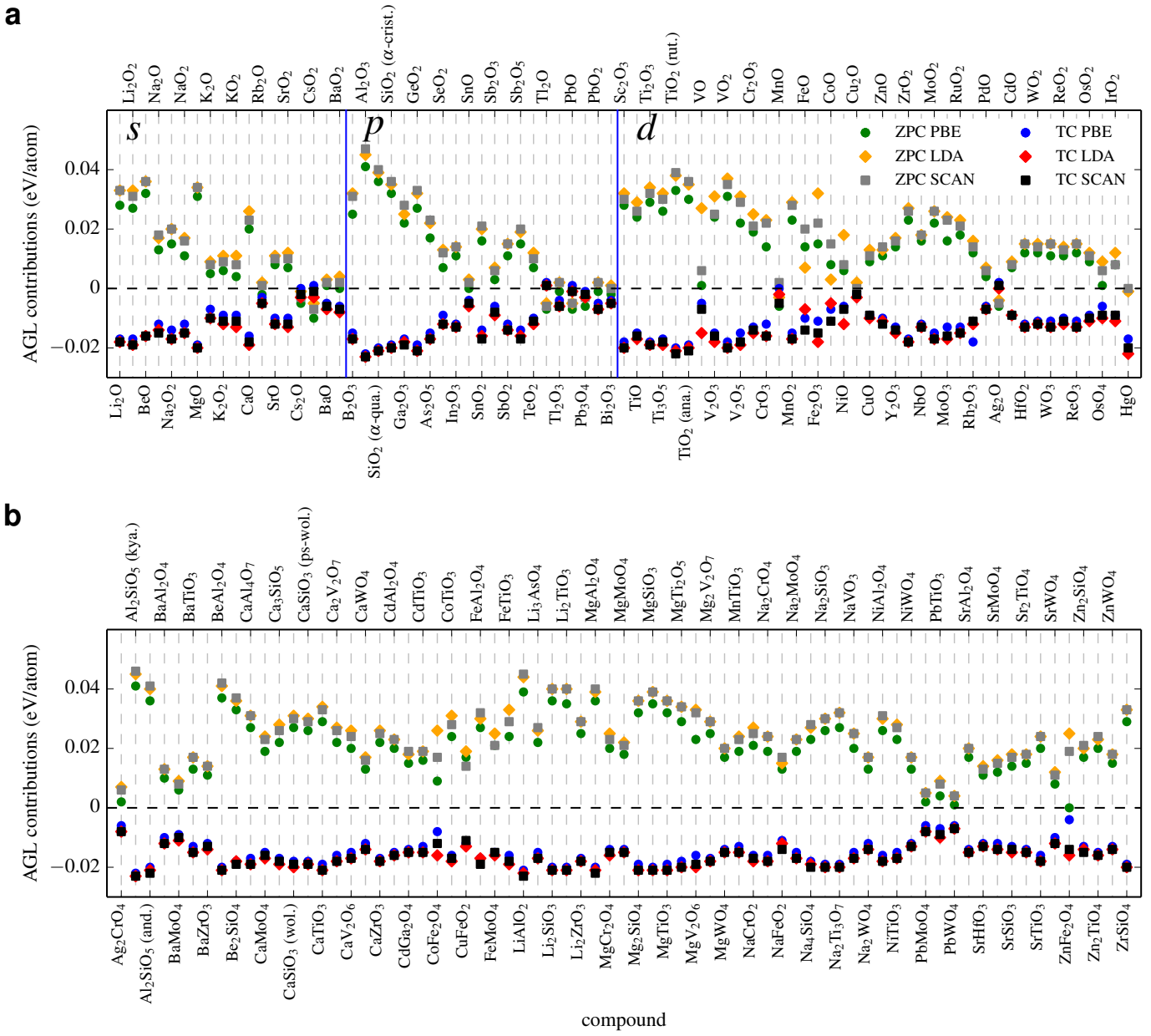

FIG. 3. **Zero-point *vs.* thermal contribution.** Comparison of the zero-point (ZPC) and thermal (TC) contributions to the room temperature formation enthalpies for binary (**a**) and ternary (**b**) oxides.

III. Comparison of the zero-point and thermal contributions to the formation enthalpy

Figures 3(a,b) depict the individual zero-point and thermal contributions to the formation enthalpy according to Eq. (4) of the main text for binary and ternary oxides, respectively. The ZPC is usually larger. Both contributions are typically about two orders of magnitude smaller than the total values of the formation enthalpies. The maximum absolute values of the zero-point contribution (thermal contribution) of 47 (23) and 46 (23) meV/atom are reached for Al_2O_3 and kyanite Al_2SiO_5 for binary and ternary oxides with SCAN, respectively. For binaries, the zero-point contribution is almost always positive (or minimally −10 meV/atom for CsO_2 for PBE), while the thermal is basically always negative (or maximally 2 meV/atom for Ag_2O and Tl_2O for PBE). For ternaries the contributions always have opposite sign leading to a partial cancellation, involving two effects: **i.** the bonds for the ionic compound (for especially light elements) are rather stiff, leading to a large zero-point vibrational energy with respect to the references, giving a positive contribution to the formation enthalpy; **ii.** for systems with stiff bonds, only a small part of the vibrational spectrum is accessible to thermal excitations, giving a negative contribution to the formation enthalpies, as the enthalpies of the elements increase more strongly with temperature than the compounds.

IV. Dependence of the oxygen correction on the fitting set

According to Wang *et al.* [6], DFT formation energies of oxides can be corrected by plotting the difference between calculated and experimental values for non-transition metal compounds, normalized to O_2 in the formula unit (Fig. 4). Here, the calculated room temperature formation enthalpies are used. In contrast, the original work considered formation energies directly calculated with DFT. The differences are negligible given the small size of the vibrational contribution. As proposed by Wang *et al.*, [6] the $\Delta_f H^{\circ,T_r,\mathrm{cal}}$ should have a rather constant shift from $\Delta_f H^{\circ,T_r,\mathrm{exp}}$, which was estimated to be 1.36 eV/O_2 for PBE, based on a fit of six non-transition metal (*s*- and *p*-) oxides. The calculated formation enthalpies could then be corrected by subtracting the value.

This is a good approximation for binary *s*-oxides (O^{2-} anions) and PBE (filled green symbols in Fig. 4): the oxygen correction fitted to the data amounts to 1.39 eV/O_2, in close agreement with the initially proposed value. However, when all *p*-oxides are included (open green symbols in Fig. 4), a constant shift is not adequate, leading to a very different correction of 0.86 eV. Also, for LDA and SCAN, when the formation enthalpies of *p*-oxides are included, the scatter increases towards lower values. The trend is less pronounced than for PBE.

When fitting the oxygen correction to the formation enthalpies of the *s*-oxides calculated for SCAN, a small value 0.06 eV is obtained. The SCAN binding energy for O_2 (−5.59 eV) is also closer to experiment (−5.12 eV) [1] than PBE (−6.05 eV) and LDA (−7.49 eV), in good agreement with previous reports [6–10]. As such, the better description of oxides by SCAN *vs.* PBE is mostly due to its improved treatment of O_2.

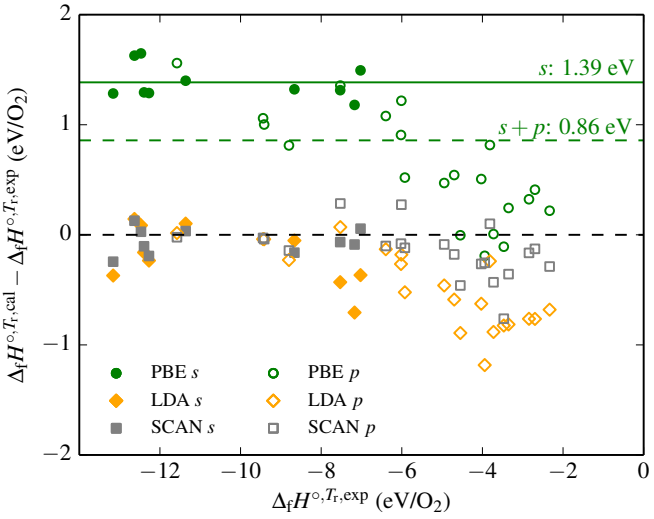

FIG. 4. **Variation of the oxygen correction.** Dependence of the oxygen correction on the set of compounds used for the fitting. The filled (open) symbols correspond to *s*-oxides (*p*-oxides). For PBE, the fitting curves are drawn with only the *s*-oxides used to obtain the correction (solid green line) and all *s*- and *p*-oxides are used (dashed green line). The scale is normalized to eV/O_2.

V. Importance of *ab-initio* data for CCE

To investigate the importance of the information included in the *ab-initio* data on the accuracy of CCE, we derive the corrections per bond from the experimental binaries and apply to the ternaries without using DFT data (CCE@exp). In Figure 5, the results are compared to the CCE corrected SCAN data (CCE@SCAN) for the test set of 71 ternary oxides. The MAE is about an order of magnitude higher, *i.e.* 244 *vs.* 27 meV/atom, when using no *ab-initio* data as input, indicating that the information obtained from DFT is essential for CCE: predicting the stability of a compound only from nearest neighbor interactions (CCE@exp) is not a very good approximation. However, the DFT error for the formation enthalpy appears to be rather well reproduced from only nearest neighbor contributions.

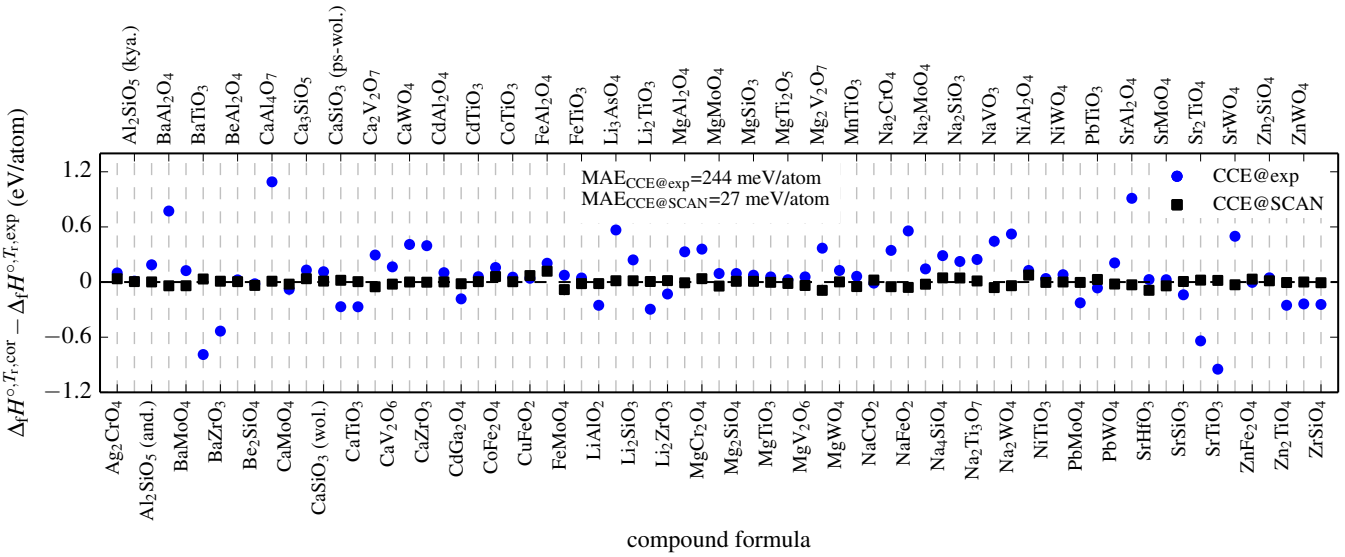

FIG. 5. **Importance of input data for CCE.** Differences between corrected and experimental room temperature formation enthalpies for the test set of 71 ternary oxides if the CCE method is based on only experimental data for binary oxides (CCE@exp), or applied on top of calculated SCAN results (CCE@SCAN).

VI. Tables with numerical data

TABLE II: **Structural data.** ICSD numbers, space group numbers and Pearson symbols for the structures of 79 binary and 71 ternary oxides. Space-groups and Pearson symbols are calculated with AFLOW-SYM [11].

formula	ICSD #	space group #	Pearson symbol	formula	ICSD #	space group #	Pearson symbol
Li_2O	642216	225	cF12	Ag_2CrO_4	16298	62	oP28
Li_2O_2	152183	194	hP8	Al_2SiO_5 (kya.)	85742	2	aP32
BeO	62736	186	hP4	Al_2SiO_5 (and.)	30679	58	oP32
Na_2O	60435	225	cF12	$BaAl_2O_4$	246027	173	hP56
Na_2O_2	25526	189	hP12	$BaMoO_4$	50821	88	tI24
NaO_2	87178	205	cP12	$BaTiO_3$	187292	221	cP5
MgO	159378	225	cF8	$BaZrO_3$	27048	221	cP5
K_2O	180571	225	cF12	$BeAl_2O_4$	34806	62	oP28
K_2O_2	180559	64	oS16	Be_2SiO_4	64945	148	hR42
KO_2	38245	139	tI6	$CaAl_4O_7$	14270	15	mS48
CaO	60704	225	cF8	$CaMoO_4$	417513	88	tI24
Rb_2O	77906	225	cF12	Ca_3SiO_5	81100	8	mS54
SrO	181061	225	cF8	$CaSiO_3$ (wol.)	201537	2	aP30
SrO_2	647474	139	tI6	$CaSiO_3$ (ps-wol.)	87694	15	mS60
Cs_2O	27919	166	hR3	$CaTiO_3$	165801	62	oP20
CsO_2	38247	139	tI6	$Ca_2V_2O_7$	421266	2	aP22
BaO	26961	225	cF8	CaV_2O_6	166516	12	mS18
BaO_2	24248	139	tI6	$CaWO_4$	60547	88	tI24
B_2O_3	24649	144	hP15	$CaZrO_3$	97463	62	oP20
Al_2O_3	89664	167	hR10	$CdAl_2O_4$	183382	227	cF56
SiO_2 (α-qua.)	79635	152	hP9	$CdGa_2O_4$	159739	227	cF56
SiO_2 (α-crist.)	153886	92	tP12	$CdTiO_3$	15989	148	hR10
Ga_2O_3	83645	12	mS20	$CoFe_2O_4$	166200	227	cF56
GeO_2	158597	136	tP6	$CoTiO_3$	48107	148	hR10
As_2O_5	654040	19	oP28	$CuFeO_2$	246912	166	hR4
SeO_2	59712	135	tP24	$FeAl_2O_4$	56117	227	cF56
In_2O_3	33649	206	cI80	$FeMoO_4$	43012	12	mS48
SnO	16481	129	tP4	$FeTiO_3$	187688	148	hR10
SnO_2	184420	136	tP6	$LiAlO_2$	28288	166	hR4
Sb_2O_3	31102	227	cF80	Li_3AsO_4	75927	31	oP16
SbO_2	4109	33	oP24	Li_2SiO_3	28192	36	oS24

TABLE II. (*continued*)

formula	ICSD #	space group #	Pearson symbol	formula	ICSD #	space group #	Pearson symbol
Sb_2O_5	1422	15	mS28	Li_2TiO_3	162215	15	mS48
TeO_2	161691	92	tP12	Li_2ZrO_3	94893	15	mS24
Tl_2O	16220	166	hR6	$MgAl_2O_4$	24766	227	cF56
Tl_2O_3	26813	206	cI80	$MgCr_2O_4$	160953	227	cF56
PbO	53927	129	tP4	$MgMoO_4$	20418	12	mS48
Pb_3O_4	29094	135	tP28	Mg_2SiO_4	83793	62	oP28
PbO_2	34234	136	tP6	$MgSiO_3$	30895	14	mP40
Bi_2O_3	168806	14	mP20	$MgTiO_3$	171792	148	hR10
Sc_2O_3	647398	206	cI80	$MgTi_2O_5$	37232	63	oS32
TiO	56694	12	mS20	MgV_2O_6	10391	12	mS18
Ti_2O_3	647550	167	hR10	$Mg_2V_2O_7$	2321	2	aP22
Ti_3O_5	75193	12	mS32	$MgWO_4$	67903	13	mP12
TiO_2 (rut.)	33837	136	tP6	$MnTiO_3$	171579	148	hR10
TiO_2 (ana.)	154602	141	tI12	$NaCrO_2$	182235	166	hR4
VO	647627	225	cF8	Na_2CrO_4	76001	63	oS28
V_2O_3	94768	167	hR10	$NaFeO_2$	186309	33	oP16
VO_2	647610	14	mP12	Na_2MoO_4	151970	227	cF56
V_2O_5	60767	59	oP14	Na_4SiO_4	15500	2	aP18
Cr_2O_3	167268	167	hR10	Na_2SiO_3	24664	36	oS24
CrO_3	16031	40	oS16	$Na_2Ti_3O_7$	15463	11	mP24
MnO	53928	225	cF8	$NaVO_3$	2103	15	mS40
MnO_2	20229	136	tP6	Na_2WO_4	44524	227	cF56
FeO	31081	225	cF8	$NiAl_2O_4$	608815	227	cF56
Fe_2O_3	201097	167	hR10	$NiTiO_3$	33855	148	hR10
CoO	9865	225	cF8	$NiWO_4$	16685	13	mP12
NiO	166115	225	cF8	$PbMoO_4$	89034	88	tI24
Cu_2O	628619	224	cP6	$PbTiO_3$	162046	99	tP5
CuO	92368	15	mS8	$PbWO_4$	93374	88	tI24
ZnO	163380	186	hP4	$SrAl_2O_4$	160297	4	mP28
Y_2O_3	27772	206	cI80	$SrHfO_3$	84280	62	oP20
ZrO_2	80043	14	mP12	$SrMoO_4$	23700	88	tI24
NbO	27574	221	cP6	$SrSiO_3$	32542	5	mS60
MoO_2	644064	14	mP12	Sr_2TiO_4	157402	139	tI14
MoO_3	151751	62	oP16	$SrTiO_3$	187296	221	cP5
RuO_2	647377	136	tP6	$SrWO_4$	23701	88	tI24
Rh_2O_3	181829	167	hR10	$ZnFe_2O_4$	91935	227	cF56
PdO	26598	131	tP4	Zn_2SiO_4	20093	148	hR42
Ag_2O	174091	224	cP6	Zn_2TiO_4	109093	91	tP28
CdO	181294	225	cF8	$ZnWO_4$	156482	13	mP12
HfO_2	173158	14	mP12	$ZrSiO_4$	71942	141	tI24
WO_2	8217	14	mP12				
WO_3	84848	14	mP16				
ReO_2	647349	14	mP12				
ReO_3	16810	221	cP4				
OsO_2	647244	136	tP6				
OsO_4	23803	15	mS20				
IrO_2	640887	136	tP6				
HgO	14124	62	oP8				

TABLE III: **Structural data for halides.** ICSD numbers, space group numbers and Pearson symbols for the structures of 9 binary and 7 ternary halides. Space-groups and Pearson symbols are calculated with AFLOW-SYM [11].

formula	ICSD #	space group #	Pearson symbol	formula	ICSD #	space group #	Pearson symbol
LiF	44272	225	cF8	KBF_4	22260	62	oP24
NaF	52238	225	cF8	Li_3AlF_6	85171	15	mS120
KF	64686	225	cF8	Li_2BeF_4	72423	148	hR42
BeF_2	261194	152	hP9	Na_3AlF_6	30201	14	mP20
AlF_3	36034	167	hR8	$NaBF_4$	30435	63	oS24
NaCl	162800	225	cF8	Na_2SiF_6	61274	150	hP27
KCl	240527	225	cF8	$NaAlCl_4$	71159	19	oP24
$CaCl_2$	246416	58	oP6				
$AlCl_3$	39566	12	mS16				

TABLE IV: **Formation enthalpies and CCE corrections for binary oxides.** Calculated and experimental room temperature formation enthalpies, corrections per bond $\delta H_{A-O}^{A^{+\alpha}}$, number of cation-oxygen bonds N_{A-O} per formula unit and oxidation states $+\alpha$ of the cation for binary oxides. Experimental values from Kubaschewski *et al.* [3], NIST-JANAF [1] and Barin [4]. Values in brackets denote cases in which the corrections are applied to calculate corrected values (see section II of the main text for details). The O-O bond correction for peroxides is obtained from Li_2O_2. The O-O bond correction for superoxides is derived from KO_2. The two values are listed in the table at the position of the respective compound. Enthalpies in eV/atom; corrections in eV/bond.

formula	PBE+AGL	LDA+AGL	SCAN+AGL	Exp.	$\delta H_{A-O}^{A^{+\alpha}}$ PBE+AGL	$\delta H_{A-O}^{A^{+\alpha}}$ LDA+AGL	$\delta H_{A-O}^{A^{+\alpha}}$ SCAN+AGL	N_{A-O}	$+\alpha$
Li_2O	−1.850	−2.092	−2.083	−2.066 [3]	0.0809	−0.0100	−0.0065	8	+1
Li_2O_2	−1.426	−1.704	−1.605	−1.643 [3]	−0.1050	−0.1270	0.2270	12	+1
BeO	−2.751	−3.122	−3.126	−3.158 [3]	0.2035	0.0180	0.0160	4	+2
Na_2O	−1.224	−1.453	−1.471	−1.444 [1]	0.0826	−0.0033	−0.0101	8	+1
Na_2O_2	−1.083	−1.350	−1.285	−1.329 [3]	(−1.304)	(−1.309)	(−1.311)	12	+1
NaO_2	−0.795	−1.014	−0.893	−0.901 [3]	(−0.777)	(−0.918)	(−0.856)	6	+1
MgO	−2.705	−3.096	−3.111	−3.118 [3]	0.1373	0.0072	0.0023	6	+2
K_2O	−1.036	−1.326	−1.266	−1.255 [3]	0.0821	−0.0269	−0.0041	8	+1
K_2O_2	−1.074	−1.387	−1.256	−1.282 [3]	(−1.294)	(−1.275)	(−1.300)	12	+1
KO_2	−0.893	−1.162	−1.014	−0.983 [3]	−0.5500	−0.2680	−0.0520	10	+1
CaO	−2.969	−3.382	−3.351	−3.290 [3]	0.1070	−0.0308	−0.0203	6	+2
Rb_2O	−0.922	−1.232	−1.161	−1.171 [3]	0.0934	−0.0229	0.0035	8	+1
SrO	−2.746	−3.127	−3.116	−3.068 [3]	0.1073	−0.0195	−0.0160	6	+2
SrO_2	−1.902	−2.314	−2.177	−2.189 [3]	(−2.224)	(−2.207)	(−2.199)	10	+2
Cs_2O	−0.999	−1.313	−1.210	−1.195 [3]	0.0983	−0.0588	−0.0073	6	+1
CsO_2	−0.899	−1.175	−1.011	−0.989 [3]	(−1.043)	(−0.890)	(−0.969)	10	+1
BaO	−2.490	−2.815	−2.832	−2.841 [3]	0.1167	0.0085	0.0028	6	+2
BaO_2	−1.866	−2.255	−2.128	−2.191 [3]	(−2.220)	(−2.241)	(−2.213)	10	+2
B_2O_3	−2.396	−2.708	−2.683	−2.640 [3]	0.2030	−0.0572	−0.0357	6	+3
Al_2O_3	−3.005	−3.469	−3.480	−3.473 [3]	0.1950	0.0020	−0.0028	12	+3
SiO_2 (α-qua.)	−2.794	−3.160	−3.156	−3.147 [3]	0.2648	−0.0098	−0.0070	4	+4
SiO_2 (α-crist.)	−2.804	−3.151	−3.151	−3.138 [3]	(−3.157)	(−3.138)	(−3.142)	4	+4
Ga_2O_3	−1.851	−2.237	−2.172	−2.258 [3]	0.2034	0.0105	0.0427	10	+3
GeO_2	−1.598	−2.064	−1.912	−2.004 [3]	0.2030	−0.0300	0.0457	6	+4
As_2O_5	−1.071	−1.448	−1.326	−1.362 [3]	0.2039	−0.0599	0.0251	10	+5
SeO_2	−0.705	−1.004	−0.874	−0.778 [3]	0.0730	−0.2267	−0.0960	3	+4
In_2O_3	−1.595	−1.958	−1.950	−1.919 [3]	0.1349	−0.0163	−0.0127	12	+3
SnO	−1.351	−1.611	−1.510	−1.481 [4]	0.0650	−0.0653	−0.0148	4	+2
SnO_2	−1.704	−2.095	−2.033	−2.007 [4]	0.1512	−0.0442	−0.0133	6	+4
Sb_2O_3	−1.343	−1.622	−1.511	−1.484 [3]	0.1177	−0.1150	−0.0218	6	+3
SbO_2	−1.386	−1.763	−1.626	−1.567 [3]	(−1.570)	(−1.556)	(−1.556)	5	+3, +5
Sb_2O_5	−1.258	−1.663	−1.533	−1.439 [4]	0.1056	−0.1304	−0.0551	12	+5
TeO_2	−1.036	−1.389	−1.236	−1.117 [4]	0.0610	−0.2035	−0.0893	4	+4
Tl_2O	−0.596	−0.716	−0.705	−0.578 [3]	−0.0090	−0.0687	−0.0635	6	+1
Tl_2O_3	−0.686	−1.038	−0.847	−0.809 [3]	0.0513	−0.0955	−0.0159	12	+3
PbO	−1.138	−1.360	−1.252	−1.137 [3]	−0.0005	−0.1115	−0.0575	4	+2
Pb_3O_4	−1.062	−1.316	−1.187	−1.064 [3]	(−1.108)	(−1.112)	(−1.115)	12	+2, +4
PbO_2	−0.841	−1.203	−1.003	−0.948 [3]	0.0538	−0.1272	−0.0273	6	+4
Bi_2O_3	−1.240	−1.538	−1.259	−1.183 [3]	−0.0286	−0.1775	−0.0381	10	+3
Sc_2O_3	−3.558	−3.964	−4.006	−3.956 [3]	0.1656	−0.0034	−0.0212	12	+3
TiO	−2.532	−2.961	−2.865	−2.812 [3]	0.1169	−0.0619	−0.0221	4.8	+2
Ti_2O_3	−2.907	−3.344	−3.304	−3.153 [3]	0.1025	−0.0796	−0.0633	12	+3
Ti_3O_5	−2.966	−3.360	−3.364	−3.186 [3]	(−3.205)	(−3.174)	(−3.183)	18	+3, +4
TiO_2 (rut.)	−3.034	−3.438	−3.491	−3.261 [3]	0.1138	−0.0882	−0.1150	6	+4
TiO_2 (ana.)	−3.067	−3.449	−3.502	−3.243 [1]	(−3.295)	(−3.273)	(−3.272)	6	+4
VO	−1.450	−1.865	−1.767	−2.237 [3]	0.2623	0.1240	0.1568	6	+2
V_2O_3	−2.282	−2.672	−2.646	−2.526 [3]	0.1018	−0.0608	−0.0498	12	+3
VO_2	−2.360	−2.749	−2.758	−2.466 [3]	0.0528	−0.1413	−0.1462	6	+4
V_2O_5	−2.301	−2.586	−2.595	−2.295 [3]	−0.0037	−0.2033	−0.2101	10	+5
Cr_2O_3	−1.979	−2.233	−2.390	−2.352 [3]	0.1553	0.0495	−0.0159	12	+3
CrO_3	−1.651	−1.819	−1.796	−1.521 [3]	−0.1305	−0.2980	−0.2745	4	+6
MnO	−1.247	−1.190	−2.095	−1.994 [3]	0.2492	0.2682	−0.0333	6	+2
MnO_2	−1.672	−1.977	−2.105	−1.800 [3]	0.0640	−0.0885	−0.1528	6	+4
FeO	−0.877	−1.016	−1.347	−1.410 [1]	0.1775	0.1312	0.0210	6	+2

TABLE IV. (*continued*)

formula	PBE+AGL	LDA+AGL	SCAN+AGL	Exp.	$\delta H_{A-\mathrm{O}}^{A^{+\alpha}}$ PBE+AGL	$\delta H_{A-\mathrm{O}}^{A^{+\alpha}}$ LDA+AGL	$\delta H_{A-\mathrm{O}}^{A^{+\alpha}}$ SCAN+AGL	$N_{A-\mathrm{O}}$	$+\alpha$
Fe_2O_3	−1.311	−1.662	−1.857	−1.707 [3]	0.1648	0.0187	−0.0625	12	+3
CoO	−0.512	−0.736	−0.859	−1.232 [3]	0.2398	0.1655	0.1243	6	+2
NiO	−0.475	−0.770	−0.647	−1.242 [3]	0.2555	0.1572	0.1982	6	+2
Cu_2O	−0.417	−0.546	−0.507	−0.590 [1]	0.1293	0.0328	0.0618	4	+1
CuO	−0.605	−0.858	−0.793	−0.808 [1]	0.1018	−0.0245	0.0075	4	+2
ZnO	−1.445	−1.730	−1.723	−1.817 [3]	0.1858	0.0433	0.0468	4	+2
Y_2O_3	−3.622	−3.999	−4.063	−3.949 [3]	0.1363	−0.0209	−0.0474	12	+3
ZrO_2	−3.460	−3.888	−3.931	−3.791 [1]	0.1419	−0.0416	−0.0597	7	+4
NbO	−2.053	−2.422	−2.339	−2.175 [3]	0.0610	−0.1235	−0.0820	4	+2
MoO_2	−1.966	−2.390	−2.233	−2.031 [3]	0.0327	−0.1797	−0.1008	6	+4
MoO_3	−1.975	−2.264	−2.180	−1.931 [3]	−0.0440	−0.3335	−0.2490	4	+6
RuO_2	−1.059	−1.458	−1.271	−1.054 [3]	−0.0027	−0.2020	−0.1085	6	+4
Rh_2O_3	−0.710	−1.060	−0.874	−0.737 [3]	0.0115	−0.1347	−0.0572	12	+3
PdO	−0.485	−0.757	−0.648	−0.599 [3]	0.0568	−0.0793	−0.0250	4	+2
Ag_2O	−0.123	−0.183	−0.198	−0.107 [3]	−0.0115	−0.0568	−0.0683	4	+1
CdO	−1.028	−1.292	−1.324	−1.339 [3]	0.1037	0.0158	0.0050	6	+2
HfO_2	−3.577	−4.022	−4.016	−3.955 [4]	0.1617	−0.0290	−0.0263	7	+4
WO_2	−1.923	−2.352	−2.131	−2.037 [3]	0.0570	−0.1575	−0.0473	6	+4
WO_3	−2.176	−2.493	−2.385	−2.183 [3]	0.0052	−0.2063	−0.1347	6	+6
ReO_2	−1.371	−1.797	−1.507	−1.551 [4]	0.0898	−0.1230	0.0218	6	+4
ReO_3	−1.635	−1.980	−1.764	−1.526 [4]	−0.0722	−0.3027	−0.1582	6	+6
OsO_2	−0.895	−1.305	−1.015	−1.018 [3]	0.0613	−0.1438	0.0015	6	+4
OsO_4	−0.999	−1.120	−1.040	−0.816 [3]	−0.2288	−0.3805	−0.2803	4	+8
IrO_2	−0.799	−1.200	−0.803	−0.838 [4]	0.0198	−0.1808	0.0177	6	+4
HgO	−0.319	−0.557	−0.433	−0.470 [3]	0.1515	−0.0870	0.0375	2	+2

TABLE V: **Formation enthalpies and CCE corrections for binary halides.** Calculated and experimental room temperature formation enthalpies, corrections per bond $\delta H_{A-X}^{A^{+\alpha}}$, number of cation-anion bonds N_{A-X} per formula unit and oxidation states $+\alpha$ of the cation for binary halides. Experimental values from Kubaschewski *et al.* [3] and NIST-JANAF [1]. Note that BF_3 and SiF_4 are gaseous molecular systems. Enthalpies in eV/atom; corrections in eV/bond.

formula	PBE+AGL	LDA+AGL	SCAN+AGL	Exp.	$\delta H_{A-X}^{A^{+\alpha}}$ PBE+AGL	$\delta H_{A-X}^{A^{+\alpha}}$ LDA+AGL	$\delta H_{A-X}^{A^{+\alpha}}$ SCAN+AGL	N_{A-X}	$+\alpha$
LiF	−2.960	−3.161	−3.342	−3.197 [1]	0.0788	0.0120	−0.0482	6	+1
NaF	−2.732	−2.904	−3.124	−2.982 [1]	0.0833	0.0258	−0.0473	6	+1
KF	−2.731	−2.922	−3.088	−2.946 [1]	0.0718	0.0083	−0.0472	6	+1
BeF_2	−3.271	−3.472	−3.709	−3.547 [3]	0.2073	0.0563	−0.1215	4	+2
BF_3(g)	−2.760	−2.824	−3.067	−2.943 [3]	0.2447	0.1587	−0.1640	3	+3
AlF_3	−3.540	−3.828	−4.095	−3.913 [3]	0.2488	0.0572	−0.1208	6	+3
SiF_4(g)	−3.097	−3.208	−3.470	−3.348 [3]	0.3135	0.1750	−0.1525	4	+4
NaCl	−1.832	−1.961	−2.077	−2.131 [3]	0.1000	0.0568	0.0180	6	+1
KCl	−1.981	−2.116	−2.212	−2.263 [3]	0.0938	0.0488	0.0168	6	+1
$CaCl_2$	−2.425	−2.598	−2.701	−2.747 [3]	0.1608	0.0742	0.0227	6	+2
$AlCl_3$	−1.538	−1.753	−1.755	−1.828 [3]	0.1933	0.0498	0.0485	6	+3

TABLE VI: **Uncorrected and CCE corrected formation enthalpies for ternary oxides.** Calculated, coordination corrected and experimental room temperature formation enthalpies, number of cation-oxygen bonds $N_{1/2-\mathrm{O}}$ per formula unit and oxidation states $+\alpha$ of the cations for ternary oxides. For the cation-oxygen bonds- and oxidation numbers, the first (second) number in the column refers to the first (second) element in the formula. Experimental values from Kubaschewski *et al.* [3], NIST-JANAF [1] and Barin [4]. Enthalpies in eV/atom.

formula	PBE+AGL	LDA+AGL	SCAN+AGL	PBE+AGL CCE	LDA+AGL CCE	SCAN+AGL CCE	Exp.	$N_{1/2-\mathrm{O}}$	$+\alpha$
Ag_2CrO_4	−1.104	−1.285	−1.302	−1.013	−1.033	−1.047	−1.083 [4]	10, 4	+1, +6
Al_2SiO_5 (kya.)	−2.917	−3.365	−3.363	−3.342	−3.364	−3.356	−3.361 [1]	12, 4	+3, +4
Al_2SiO_5 (and.)	−2.940	−3.354	−3.364	−3.340	−3.352	−3.357	−3.358 [1]	11, 4	+3, +4
$BaAl_2O_4$	−3.065	−3.402	−3.482	−3.413	−3.413	−3.482	−3.441 [3]	7.5, 8	+2, +3
$BaMoO_4$	−2.616	−2.872	−2.876	−2.742	−2.661	−2.714	−2.674 [4]	8, 4	+2, +6
$BaTiO_3$	−3.090	−3.526	−3.538	−3.506	−3.440	−3.407	−3.441 [4]	12, 6	+2, +4
$BaZrO_3$	−3.302	−3.696	−3.744	−3.752	−3.667	−3.679	−3.689 [4]	12, 6	+2, +4

TABLE VI. (*continued*)

formula	PBE+AGL	LDA+AGL	SCAN+AGL	PBE+AGL CCE	LDA+AGL CCE	SCAN+AGL CCE	Exp.	$N_{1/2-O}$	$+\alpha$
$BeAl_2O_4$	−2.953	−3.385	−3.398	−3.403	−3.399	−3.402	−3.407 [3]	4, 12	+2, +3
Be_2SiO_4	−2.778	−3.161	−3.157	−3.162	−3.176	−3.171	−3.134 [1]	8, 4	+2, +4
$CaAl_4O_7$	−3.064	−3.413	−3.480	−3.368	−3.403	−3.468	−3.477 [4]	5, 16	+2, +3
$CaMoO_4$	−2.594	−2.915	−2.886	−2.707	−2.652	−2.693	−2.671 [3]	8, 4	+2, +6
Ca_3SiO_5	−3.002	−3.395	−3.380	−3.334	−3.329	−3.336	−3.373 [3]	18, 4	+2, +4
$CaSiO_3$ (wol.)	−3.038	−3.412	−3.410	−3.385	−3.366	−3.379	−3.389 [3]	$6.\overline{3}$, 4	+2, +4
$CaSiO_3$ (ps-wol.)	−3.018	−3.391	−3.393	−3.401	−3.334	−3.355	−3.375 [3]	8, 4	+2, +4
$CaTiO_3$	−3.163	−3.591	−3.608	−3.471	−3.436	−3.438	−3.442 [3]	8, 6	+2, +4
$Ca_2V_2O_7$	−2.804	−3.118	−3.152	−2.928	−2.915	−2.956	−2.905 [3]	13, 9	+2, +5
CaV_2O_6	−2.642	−2.918	−2.951	−2.709	−2.671	−2.704	−2.682 [3]	6, 10	+2, +5
$CaWO_4$	−2.661	−2.984	−2.958	−2.807	−2.805	−2.841	−2.842 [4]	8, 4	+2, +6
$CaZrO_3$	−3.329	−3.727	−3.759	−3.628	−3.640	−3.663	−3.662 [3]	6, 6	+2, +4
$CdAl_2O_4$	−2.438	−2.834	−2.838	−2.831	−2.846	−2.837	−2.838 [3]	4, 12	+2, +3
$CdGa_2O_4$	−1.645	−1.999	−1.949	−2.053	−2.026	−2.025	−2.007 [3]	4, 12	+2, +3
$CdTiO_3$	−2.289	−2.629	−2.678	−2.550	−2.542	−2.546	−2.551 [4]	6, 6	+2, +4
$CoFe_2O_4$	−1.143	−1.458	−1.588	−1.562	−1.585	−1.552	−1.612 [3]	4, 12	+2, +3
$CoTiO_3$	−2.089	−2.418	−2.488	−2.514	−2.511	−2.499	−2.503 [3]	6, 6	+2, +4
$CuFeO_2$	−0.920	−1.275	−1.321	−1.232	−1.319	−1.258	−1.329 [3]	2, 6	+1, +3
$FeAl_2O_4$	−2.400	−2.740	−2.829	−2.836	−2.819	−2.836	−2.954 [4]	4, 12	+2, +3
$FeMoO_4$	−1.637	−2.036	−2.058	−1.785	−1.945	−1.913	−1.831 [3]	6, 4	+2, +6
$FeTiO_3$	−2.231	−2.506	−2.695	−2.580	−2.557	−2.582	−2.565 [3]	6, 6	+2, +4
$LiAlO_2$	−2.720	−3.101	−3.111	−3.133	−3.089	−3.096	−3.080 [3]	6, 6	+1, +3
Li_3AsO_4	−1.939	−2.200	−2.188	−2.162	−2.155	−2.191	−2.205 [4]	12, 4	+1, +5
Li_2SiO_3	−2.545	−2.848	−2.847	−2.829	−2.828	−2.834	−2.848 [3]	8, 4	+1, +4
Li_2TiO_3	−2.653	−2.986	−3.006	−2.929	−2.878	−2.878	−2.884 [3]	12, 6	+1, +4
Li_2ZrO_3	−2.759	−3.076	−3.101	−3.063	−3.015	−3.028	−3.044 [3]	12, 6	+1, +4
$MgAl_2O_4$	−2.976	−3.393	−3.415	−3.388	−3.401	−3.412	−3.404 [1]	4, 12	+2, +3
$MgCr_2O_4$	−2.225	−2.458	−2.621	−2.569	−2.547	−2.595	−2.632 [3]	4, 12	+2, +3
$MgMoO_4$	−2.371	−2.634	−2.626	−2.479	−2.419	−2.463	−2.419 [3]	6, 4	+2, +6
Mg_2SiO_4	−2.825	−3.203	−3.215	−3.212	−3.209	−3.215	−3.223 [3]	12, 4	+2, +4
$MgSiO_3$	−2.812	−3.203	−3.204	−3.188	−3.203	−3.202	−3.210 [3]	6, 4	+2, +4
$MgTiO_3$	−2.971	−3.357	−3.398	−3.272	−3.260	−3.263	−3.260 [3]	6, 6	+2, +4
$MgTi_2O_5$	−3.018	−3.389	−3.437	−3.291	−3.262	−3.266	−3.251 [1]	6, 12	+2, +4
MgV_2O_6	−2.479	−2.783	−2.804	−2.567	−2.562	−2.572	−2.534 [3]	6, 10	+2, +5
$Mg_2V_2O_7$	−2.573	−2.866	−2.911	−2.720	−2.726	−2.761	−2.671 [3]	12, 8	+2, +5
$MgWO_4$	−2.446	−2.801	−2.751	−2.589	−2.602	−2.619	−2.621 [3]	6, 6	+2, +6
$MnTiO_3$	−2.441	−2.639	−3.044	−2.877	−2.855	−2.866	−2.817 [3]	6, 6	+2, +4
$NaCrO_2$	−1.900	−2.118	−2.288	−2.257	−2.187	−2.249	−2.271 [3]	6, 6	+1, +3
Na_2CrO_4	−1.976	−2.179	−2.209	−2.019	−2.004	−2.037	−1.987 [4]	10, 4	+1, +6
$NaFeO_2$	−1.552	−1.714	−1.940	−1.800	−1.730	−1.867	−1.809 [3]	4, 4	+1, +3
Na_2MoO_4	−2.120	−2.346	−2.358	−2.236	−2.149	−2.198	−2.175 [4]	12, 4	+1, +6
Na_4SiO_4	−2.093	−2.373	−2.397	−2.376	−2.362	−2.374	−2.420 [3]	18, 4	+1, +4
Na_2SiO_3	−2.361	−2.657	−2.677	−2.675	−2.645	−2.656	−2.700 [3]	10, 4	+1, +4
$Na_2Ti_3O_7$	−2.787	−3.116	−3.167	−3.017	−2.989	−2.995	−3.007 [3]	10, 17	+1, +4
$NaVO_3$	−2.345	−2.556	−2.619	−2.442	−2.389	−2.439	−2.379 [4]	6, 4	+1, +5
Na_2WO_4	−2.175	−2.397	−2.417	−2.319	−2.273	−2.322	−2.283 [3]	12, 4	+1, +6
$NiAl_2O_4$	−2.279	−2.641	−2.659	−2.759	−2.735	−2.768	−2.844 [3]	4, 12	+2, +3
$NiTiO_3$	−2.070	−2.398	−2.396	−2.513	−2.481	−2.496	−2.492 [3]	6, 6	+2, +4
$NiWO_4$	−1.659	−1.980	−1.886	−1.920	−1.931	−1.949	−1.950 [3]	6, 6	+2, +6
$PbMoO_4$	−1.893	−2.134	−2.066	−1.863	−1.763	−1.823	−1.819 [3]	8, 4	+2, +6
$PbTiO_3$	−2.350	−2.685	−2.655	−2.463	−2.418	−2.448	−2.476 [3]	8, 5	+2, +4
$PbWO_4$	−1.948	−2.187	−2.125	−1.951	−1.901	−1.958	−1.937 [3]	8, 4	+2, +6
$SrAl_2O_4$	−3.074	−3.419	−3.489	−3.389	−3.405	−3.472	−3.442 [4]	6, 8	+2, +3
$SrHfO_3$	−3.416	−3.826	−3.844	−3.782	−3.760	−3.787	−3.697 [3]	8, 6	+2, +4
$SrMoO_4$	−2.624	−2.918	−2.905	−2.738	−2.670	−2.717	−2.676 [3]	8, 4	+2, +6
$SrSiO_3$	−3.039	−3.401	−3.411	−3.422	−3.362	−3.380	−3.386 [3]	8, 4	+2, +4
Sr_2TiO_4	−3.074	−3.492	−3.506	−3.447	−3.366	−3.366	−3.387 [3]	18, 6	+2, +4
$SrTiO_3$	−3.164	−3.596	−3.622	−3.558	−3.444	−3.445	−3.463 [3]	12, 6	+2, +4
$SrWO_4$	−2.688	−2.981	−2.973	−2.834	−2.818	−2.862	−2.832 [4]	8, 4	+2, +6
$ZnFe_2O_4$	−1.288	−1.669	−1.783	−1.676	−1.726	−1.703	−1.735 [4]	4, 12	+2, +3
Zn_2SiO_4	−2.054	−2.376	−2.370	−2.417	−2.420	−2.419	−2.433 [3]	8, 4	+2, +4

TABLE VI. (*continued*)

formula	PBE+AGL	LDA+AGL	SCAN+AGL	PBE+AGL CCE	LDA+AGL CCE	SCAN+AGL CCE	Exp.	$N_{1/2-O}$	$+\alpha$
Zn_2TiO_4	−2.115	−2.457	−2.479	−2.478	−2.444	−2.448	−2.443 [3]	10, 6	+2, +4
$ZnWO_4$	−1.937	−2.282	−2.214	−2.128	−2.119	−2.126	−2.126 [3]	6, 6	+2, +6
$ZrSiO_4$	−3.146	−3.579	−3.587	−3.511	−3.518	−3.503	−3.496 [1]	8, 4	+4, +4

TABLE VII: **Uncorrected and CCE corrected formation enthalpies for ternary halides.** Calculated, coordination corrected and experimental room temperature formation enthalpies, number of cation-anion bonds $N_{1/2-X}$ per formula unit and oxidation states $+\alpha$ of the cations for ternary halides. For the cation-oxygen bonds- and oxidation numbers, the first (second) number in the column refers to the first (second) element in the formula. Experimental values from Kubaschewski *et al.* [3] and NIST-JANAF [1]. Enthalpies in eV/atom.

formula	PBE+AGL	LDA+AGL	SCAN+AGL	PBE+AGL CCE	LDA+AGL CCE	SCAN+AGL CCE	Exp.	$N_{1/2-X}$	$+\alpha$
KBF_4	−3.035	−3.235	−3.425	−3.318	−3.354	−3.237	−3.255 [3]	10, 4	+1, +3
Li_3AlF_6	−3.231	−3.443	−3.663	−3.485	−3.494	−3.526	−3.507 [1]	$13.\overline{3}$, 6	+1, +3
Li_2BeF_4	−3.135	−3.299	−3.512	−3.344	−3.345	−3.388	−3.365 [3]	8, 4	+1, +2
Na_3AlF_6	−3.079	−3.267	−3.508	−3.361	−3.343	−3.359	−3.433 [3]	16, 6	+1, +3
$NaBF_4$	−2.961	−3.150	−3.349	−3.235	−3.290	−3.177	−3.187 [3]	8, 4	+1, +3
Na_2SiF_6	−3.088	−3.316	−3.518	−3.408	−3.467	−3.353	−3.354 [3]	12, 6	+1, +4
$NaAlCl_4$	−1.696	−1.816	−1.904	−1.909	−1.896	−1.952	−1.973 [1]	5, 4	+1, +3

TABLE VIII: **Uncorrected and quasi-FERE corrected formation enthalpies for ternary oxides.** Calculated, quasi-FERE corrected and experimental room temperature formation enthalpies for ternary oxides. Experimental values from Kubaschewski *et al.* [3], NIST-JANAF [1] and Barin [4]. Enthalpies in eV/atom.

formula	PBE+AGL	LDA+AGL	SCAN+AGL	PBE+AGL quasi-FERE corr.	LDA+AGL quasi-FERE corr.	SCAN+AGL quasi-FERE corr.	Exp.
Ag_2CrO_4	−1.104	−1.285	−1.302	−1.153	−1.167	−1.163	−1.083 [4]
Al_2SiO_5 (kya.)	−2.917	−3.365	−3.363	−3.339	−3.364	−3.355	−3.361 [1]
Al_2SiO_5 (and.)	−2.940	−3.354	−3.364	−3.361	−3.352	−3.355	−3.358 [1]
$BaAl_2O_4$	−3.065	−3.402	−3.482	−3.534	−3.431	−3.516	−3.441 [3]
$BaMoO_4$	−2.616	−2.872	−2.876	−2.757	−2.660	−2.760	−2.674 [4]
$BaTiO_3$	−3.090	−3.526	−3.538	−3.381	−3.430	−3.476	−3.441 [4]
$BaZrO_3$	−3.302	−3.696	−3.744	−3.689	−3.674	−3.715	−3.689 [4]
$BeAl_2O_4$	−2.953	−3.385	−3.398	−3.403	−3.399	−3.402	−3.407 [3]
Be_2SiO_4	−2.778	−3.161	−3.157	−3.158	−3.176	−3.170	−3.134 [1]
$CaAl_4O_7$	−3.064	−3.413	−3.480	−3.507	−3.402	−3.464	−3.477 [4]
$CaMoO_4$	−2.594	−2.915	−2.886	−2.684	−2.642	−2.704	−2.671 [3]
Ca_3SiO_5	−3.002	−3.395	−3.380	−3.330	−3.329	−3.336	−3.373 [3]
$CaSiO_3$ (wol.)	−3.038	−3.412	−3.410	−3.372	−3.368	−3.379	−3.389 [3]
$CaSiO_3$ (ps-wol.)	−3.018	−3.391	−3.393	−3.353	−3.346	−3.362	−3.375 [3]
$CaTiO_3$	−3.163	−3.591	−3.608	−3.394	−3.423	−3.467	−3.442 [3]
$Ca_2V_2O_7$	−2.804	−3.118	−3.152	−2.976	−2.928	−2.996	−2.905 [3]
CaV_2O_6	−2.642	−2.918	−2.951	−2.780	−2.706	−2.774	−2.682 [3]
$CaWO_4$	−2.661	−2.984	−2.958	−2.781	−2.730	−2.819	−2.842 [4]
$CaZrO_3$	−3.329	−3.727	−3.759	−3.656	−3.632	−3.651	−3.662 [3]
$CdAl_2O_4$	−2.438	−2.834	−2.838	−2.861	−2.851	−2.838	−2.838 [3]
$CdGa_2O_4$	−1.645	−1.999	−1.949	−2.024	−2.027	−2.015	−2.007 [3]
$CdTiO_3$	−2.289	−2.629	−2.678	−2.517	−2.517	−2.567	−2.551 [4]
$CoFe_2O_4$	−1.143	−1.458	−1.588	−1.629	−1.657	−1.607	−1.612 [3]
$CoTiO_3$	−2.089	−2.418	−2.488	−2.480	−2.486	−2.520	−2.503 [3]
$CuFeO_2$	−0.920	−1.275	−1.321	−1.244	−1.345	−1.279	−1.329 [3]
$FeAl_2O_4$	−2.400	−2.740	−2.829	−2.890	−2.807	−2.804	−2.954 [4]
$FeMoO_4$	−1.637	−2.036	−2.058	−1.802	−1.867	−1.873	−1.831 [3]
$FeTiO_3$	−2.231	−2.506	−2.695	−2.551	−2.463	−2.550	−2.565 [3]
$LiAlO_2$	−2.720	−3.101	−3.111	−3.120	−3.115	−3.134	−3.080 [3]
Li_3AsO_4	−1.939	−2.200	−2.188	−2.228	−2.178	−2.245	−2.205 [4]
Li_2SiO_3	−2.545	−2.848	−2.847	−2.860	−2.855	−2.877	−2.848 [3]
Li_2TiO_3	−2.653	−2.986	−3.006	−2.883	−2.891	−2.945	−2.884 [3]
Li_2ZrO_3	−2.759	−3.076	−3.101	−3.069	−3.042	−3.068	−3.044 [3]
$MgAl_2O_4$	−2.976	−3.393	−3.415	−3.428	−3.403	−3.413	−3.404 [1]

TABLE VIII. (*continued*)

formula	PBE+AGL	LDA+AGL	SCAN+AGL	PBE+AGL quasi-FERE corr.	LDA+AGL quasi-FERE corr.	SCAN+AGL quasi-FERE corr.	Exp.
$MgCr_2O_4$	−2.225	−2.458	−2.621	−2.544	−2.507	−2.568	−2.632 [3]
$MgMoO_4$	−2.371	−2.634	−2.626	−2.492	−2.399	−2.467	−2.419 [3]
Mg_2SiO_4	−2.825	−3.203	−3.215	−3.208	−3.209	−3.214	−3.223 [3]
$MgSiO_3$	−2.812	−3.203	−3.204	−3.183	−3.203	−3.200	−3.210 [3]
$MgTiO_3$	−2.971	−3.357	−3.398	−3.239	−3.234	−3.283	−3.260 [3]
$MgTi_2O_5$	−3.018	−3.389	−3.437	−3.249	−3.230	−3.292	−3.251 [1]
MgV_2O_6	−2.479	−2.783	−2.804	−2.638	−2.596	−2.642	−2.534 [3]
$Mg_2V_2O_7$	−2.573	−2.866	−2.911	−2.777	−2.718	−2.780	−2.671 [3]
$MgWO_4$	−2.446	−2.801	−2.751	−2.597	−2.585	−2.634	−2.621 [3]
$MnTiO_3$	−2.441	−2.639	−3.044	−2.753	−2.665	−2.849	−2.817 [3]
$NaCrO_2$	−1.900	−2.118	−2.288	−2.197	−2.187	−2.278	−2.271 [3]
Na_2CrO_4	−1.976	−2.179	−2.209	−2.169	−2.131	−2.153	−1.987 [4]
$NaFeO_2$	−1.552	−1.714	−1.940	−1.919	−1.796	−1.902	−1.809 [3]
Na_2MoO_4	−2.120	−2.346	−2.358	−2.244	−2.175	−2.264	−2.175 [4]
Na_4SiO_4	−2.093	−2.373	−2.397	−2.422	−2.427	−2.463	−2.420 [3]
Na_2SiO_3	−2.361	−2.657	−2.677	−2.694	−2.694	−2.723	−2.700 [3]
$Na_2Ti_3O_7$	−2.787	−3.116	−3.167	−2.997	−2.974	−3.046	−3.007 [3]
$NaVO_3$	−2.345	−2.556	−2.619	−2.502	−2.410	−2.503	−2.379 [4]
Na_2WO_4	−2.175	−2.397	−2.417	−2.324	−2.243	−2.359	−2.283 [3]
$NiAl_2O_4$	−2.279	−2.641	−2.659	−2.832	−2.779	−2.825	−2.844 [3]
$NiTiO_3$	−2.070	−2.398	−2.396	−2.480	−2.455	−2.516	−2.492 [3]
$NiWO_4$	−1.659	−1.980	−1.886	−1.928	−1.914	−1.965	−1.950 [3]
$PbMoO_4$	−1.893	−2.134	−2.066	−1.895	−1.823	−1.880	−1.819 [3]
$PbTiO_3$	−2.350	−2.685	−2.655	−2.475	−2.471	−2.508	−2.476 [3]
$PbWO_4$	−1.948	−2.187	−2.125	−1.980	−1.895	−1.981	−1.937 [3]
$SrAl_2O_4$	−3.074	−3.419	−3.489	−3.531	−3.423	−3.504	−3.442 [4]
$SrHfO_3$	−3.416	−3.826	−3.844	−3.814	−3.786	−3.835	−3.697 [3]
$SrMoO_4$	−2.624	−2.918	−2.905	−2.751	−2.676	−2.766	−2.676 [3]
$SrSiO_3$	−3.039	−3.401	−3.411	−3.416	−3.394	−3.432	−3.386 [3]
Sr_2TiO_4	−3.074	−3.492	−3.506	−3.393	−3.398	−3.462	−3.387 [3]
$SrTiO_3$	−3.164	−3.596	−3.622	−3.439	−3.465	−3.532	−3.463 [3]
$SrWO_4$	−2.688	−2.981	−2.973	−2.844	−2.758	−2.877	−2.832 [4]
$ZnFe_2O_4$	−1.288	−1.669	−1.783	−1.675	−1.751	−1.722	−1.735 [4]
Zn_2SiO_4	−2.054	−2.376	−2.370	−2.413	−2.420	−2.418	−2.433 [3]
Zn_2TiO_4	−2.115	−2.457	−2.479	−2.401	−2.413	−2.449	−2.443 [3]
$ZnWO_4$	−1.937	−2.282	−2.214	−2.074	−2.087	−2.126	−2.126 [3]
$ZrSiO_4$	−3.146	−3.579	−3.587	−3.483	−3.524	−3.512	−3.496 [1]

TABLE IX: **AGL contributions to the formation enthalpies for binary oxides.** Total vibrational (TVC), zero-point (ZPC) and thermal (TC) contributions to the calculated formation enthalpies obtained from AGL [12–16] for each functional for binary oxides. The sum of ZPC and TC might not match exactly the total AGL contribution listed due to rounding. All values in eV/atom.

formula	PBE			LDA			SCAN		
	AGL-TVC	AGL-ZPC	AGL-TC	AGL-TVC	AGL-ZPC	AGL-TC	AGL-TVC	AGL-ZPC	AGL-TC
Li_2O	0.011	0.028	−0.017	0.014	0.033	−0.018	0.014	0.033	−0.018
Li_2O_2	0.010	0.027	−0.017	0.014	0.033	−0.019	0.013	0.031	−0.019
BeO	0.017	0.032	−0.016	0.019	0.036	−0.016	0.020	0.036	−0.016
Na_2O	0.001	0.013	−0.012	0.002	0.017	−0.014	0.003	0.018	−0.015
Na_2O_2	0.001	0.015	−0.014	0.003	0.020	−0.017	0.003	0.020	−0.017
NaO_2	−0.001	0.011	−0.012	0.002	0.017	−0.015	0.001	0.016	−0.015
MgO	0.012	0.031	−0.019	0.014	0.034	−0.020	0.014	0.034	−0.020
K_2O	−0.003	0.005	−0.007	−0.001	0.009	−0.010	−0.002	0.008	−0.010
K_2O_2	−0.003	0.006	−0.009	−0.002	0.011	−0.012	−0.002	0.009	−0.011
KO_2	−0.005	0.004	−0.009	−0.002	0.011	−0.013	−0.003	0.008	−0.011
CaO	0.004	0.020	−0.016	0.007	0.026	−0.019	0.005	0.023	−0.018
Rb_2O	−0.004	−0.002	−0.003	−0.004	0.002	−0.005	−0.004	0.001	−0.005
SrO	−0.002	0.008	−0.010	−0.001	0.011	−0.012	−0.001	0.010	−0.012
SrO_2	−0.003	0.007	−0.010	−0.001	0.012	−0.013	−0.002	0.010	−0.012
Cs_2O	−0.005	−0.005	0	−0.004	−0.001	−0.003	−0.005	−0.003	−0.002
CsO_2	−0.009	−0.010	0.001	−0.008	−0.005	−0.003	−0.008	−0.007	−0.001

TABLE IX. (*continued*)

formula	PBE			LDA			SCAN		
	AGL-TVC	AGL-ZPC	AGL-TC	AGL-TVC	AGL-ZPC	AGL-TC	AGL-TVC	AGL-ZPC	AGL-TC
BaO	−0.005	0.001	−0.005	−0.004	0.003	−0.007	−0.004	0.002	−0.006
BaO_2	−0.006	0	−0.006	−0.004	0.004	−0.008	−0.005	0.002	−0.007
B_2O_3	0.009	0.025	−0.015	0.015	0.032	−0.017	0.014	0.031	−0.017
Al_2O_3	0.019	0.041	−0.022	0.022	0.045	−0.023	0.023	0.047	−0.023
SiO_2 (α-qua.)	0.016	0.036	−0.020	0.018	0.039	−0.021	0.018	0.040	−0.021
SiO_2 (α-crist.)	0.013	0.032	−0.019	0.015	0.035	−0.020	0.016	0.036	−0.020
Ga_2O_3	0.005	0.022	−0.017	0.007	0.025	−0.018	0.008	0.028	−0.019
GeO_2	0.008	0.027	−0.019	0.011	0.032	−0.021	0.012	0.033	−0.021
As_2O_5	0.003	0.017	−0.015	0.005	0.022	−0.017	0.006	0.023	−0.017
SeO_2	−0.002	0.007	−0.009	0.001	0.013	−0.012	0	0.012	−0.012
In_2O_3	−0.001	0.011	−0.012	0.001	0.014	−0.013	0.001	0.014	−0.013
SnO	−0.004	0	−0.004	−0.003	0.003	−0.006	−0.003	0.002	−0.005
SnO_2	0.001	0.016	−0.014	0.003	0.020	−0.016	0.004	0.021	−0.017
Sb_2O_3	−0.004	0.003	−0.006	−0.002	0.007	−0.009	−0.002	0.006	−0.008
SbO_2	−0.001	0.011	−0.012	0.001	0.015	−0.014	0.001	0.015	−0.014
Sb_2O_5	0.001	0.015	−0.014	0.003	0.019	−0.016	0.004	0.020	−0.017
TeO_2	−0.002	0.007	−0.010	0	0.012	−0.012	−0.001	0.010	−0.011
Tl_2O	−0.005	−0.007	0.002	−0.004	−0.005	0.001	−0.005	−0.006	0.001
Tl_2O_3	−0.006	−0.001	−0.004	−0.005	0.002	−0.006	−0.005	0.002	−0.006
PbO	−0.006	−0.007	0.001	−0.006	−0.005	−0.001	−0.006	−0.005	−0.001
Pb_3O_4	−0.006	−0.006	−0.001	−0.006	−0.003	−0.003	−0.006	−0.003	−0.002
PbO_2	−0.006	−0.001	−0.005	−0.004	0.002	−0.007	−0.005	0.002	−0.007
Bi_2O_3	−0.006	−0.002	−0.004	−0.005	0.001	−0.005	−0.005	0	−0.005
Sc_2O_3	0.009	0.028	−0.018	0.012	0.032	−0.020	0.011	0.030	−0.020
TiO	0.009	0.024	−0.015	0.012	0.029	−0.017	0.010	0.026	−0.016
Ti_2O_3	0.011	0.029	−0.018	0.014	0.034	−0.019	0.013	0.032	−0.019
Ti_3O_5	0.009	0.026	−0.017	0.013	0.032	−0.019	0.012	0.03	−0.018
TiO_2 (rut.)	0.013	0.033	−0.020	0.016	0.038	−0.021	0.017	0.039	−0.022
TiO_2 (ana.)	0.012	0.030	−0.019	0.014	0.035	−0.020	0.015	0.036	−0.021
VO	−0.004	0.001	−0.005	0.011	0.027	−0.015	0	0.006	−0.007
V_2O_3	0.008	0.024	−0.015	0.013	0.031	−0.018	0.009	0.025	−0.016
VO_2	0.012	0.031	−0.018	0.017	0.037	−0.020	0.015	0.035	−0.020
V_2O_5	0.006	0.022	−0.015	0.012	0.031	−0.019	0.011	0.029	−0.018
Cr_2O_3	0.006	0.019	−0.013	0.010	0.025	−0.015	0.007	0.021	−0.014
CrO_3	0.002	0.014	−0.012	0.007	0.023	−0.016	0.007	0.022	−0.016
MnO	−0.006	−0.006	0	−0.005	−0.003	−0.002	−0.002	0.002	−0.005
MnO_2	0.008	0.023	−0.015	0.012	0.029	−0.017	0.011	0.028	−0.017
FeO	0.004	0.014	−0.010	0	0.007	−0.007	0.006	0.020	−0.014
Fe_2O_3	0.004	0.015	−0.011	0.014	0.032	−0.018	0.007	0.022	−0.015
CoO	0.001	0.008	−0.007	−0.002	0.003	−0.005	0.004	0.015	−0.011
NiO	−0.001	0.006	−0.006	0.006	0.018	−0.012	0.001	0.008	−0.007
Cu_2O	−0.002	0	−0.002	−0.002	0.002	−0.003	−0.002	0	−0.002
CuO	0.001	0.009	−0.009	0.003	0.013	−0.010	0.002	0.011	−0.009
ZnO	0.001	0.011	−0.010	0.002	0.013	−0.011	0.003	0.014	−0.012
Y_2O_3	0.001	0.014	−0.013	0.003	0.017	−0.015	0.002	0.016	−0.014
ZrO_2	0.006	0.023	−0.017	0.008	0.027	−0.018	0.008	0.026	−0.018
NbO	0.004	0.016	−0.012	0.005	0.018	−0.013	0.005	0.018	−0.013
MoO_2	0.007	0.022	−0.015	0.009	0.026	−0.017	0.009	0.026	−0.017
MoO_3	0.003	0.016	−0.013	0.007	0.024	−0.017	0.007	0.023	−0.016
RuO_2	0.004	0.018	−0.013	0.007	0.023	−0.015	0.006	0.021	−0.015
Rh_2O_3	−0.006	0.012	−0.018	0.004	0.016	−0.012	0.003	0.014	−0.011
PdO	−0.002	0.004	−0.006	0	0.007	−0.007	−0.001	0.006	−0.007
Ag_2O	−0.004	−0.006	0.002	−0.004	−0.004	0	−0.004	−0.005	0.001
CdO	−0.002	0.007	−0.009	−0.001	0.009	−0.009	−0.001	0.008	−0.009
HfO_2	0	0.012	−0.012	0.001	0.015	−0.013	0.001	0.015	−0.013
WO_2	0.001	0.012	−0.011	0.002	0.015	−0.012	0.002	0.014	−0.012
WO_3	0	0.011	−0.011	0.002	0.015	−0.013	0.002	0.015	−0.013
ReO_2	0	0.011	−0.010	0.002	0.014	−0.012	0.002	0.013	−0.011
ReO_3	0.001	0.012	−0.011	0.002	0.015	−0.013	0.002	0.015	−0.013
OsO_2	−0.001	0.009	−0.009	0.001	0.012	−0.011	0.001	0.011	−0.010
OsO_4	−0.005	0.001	−0.006	−0.001	0.009	−0.010	−0.002	0.006	−0.009

TABLE IX. (*continued*)

formula	PBE			LDA			SCAN		
	AGL-TVC	AGL-ZPC	AGL-TC	AGL-TVC	AGL-ZPC	AGL-TC	AGL-TVC	AGL-ZPC	AGL-TC
IrO_2	−0.001	0.008	−0.009	0.001	0.012	−0.011	−0.001	0.008	−0.009
HgO	−0.019	−0.001	−0.017	−0.022	−0.001	−0.022	−0.020	0	−0.020

TABLE X: **AGL contributions to the formation enthalpies for binary halides.** Total vibrational (TVC), zero-point (ZPC) and thermal (TC) contributions to the calculated formation enthalpies obtained from AGL [12–16] for each functional for binary halides. Note that BF_3 and SiF_4 are gaseous molecular systems. The sum of ZPC and TC might not match exactly the total AGL contribution listed due to rounding. All values in eV/atom.

formula	PBE			LDA			SCAN		
	AGL-TVC	AGL-ZPC	AGL-TC	AGL-TVC	AGL-ZPC	AGL-TC	AGL-TVC	AGL-ZPC	AGL-TC
LiF	0.012	0.023	−0.011	0.015	0.029	−0.014	0.015	0.028	−0.013
NaF	0.008	0.017	−0.009	0.010	0.022	−0.013	0.009	0.022	−0.013
KF	0.005	0.010	−0.005	0.007	0.016	−0.009	0.006	0.014	−0.008
BeF_2	0.008	0.016	−0.007	0.011	0.021	−0.010	0.011	0.021	−0.009
BF_3(g)	0.026	0.034	−0.007	0.026	0.033	−0.007	0.026	0.033	−0.007
AlF_3	0.020	0.036	−0.015	0.023	0.041	−0.018	0.024	0.042	−0.018
SiF_4(g)	0.024	0.036	−0.012	0.024	0.036	−0.012	0.024	0.035	−0.011
NaCl	0.008	0.009	−0.001	0.009	0.013	−0.004	0.009	0.011	−0.002
KCl	0.008	0.007	0	0.008	0.011	−0.003	0.008	0.010	−0.002
$CaCl_2$	0.011	0.012	0	0.013	0.016	−0.003	0.012	0.014	−0.002
$AlCl_3$	0.013	0.014	−0.001	0.015	0.019	−0.004	0.015	0.018	−0.003

TABLE XI: **AGL contributions to the formation enthalpies for ternary oxides.** Total vibrational (TVC), zero-point (ZPC) and thermal (TC) contributions to the calculated formation enthalpies obtained from AGL [12–16] for each functional for ternary oxides. The sum of ZPC and TC might not match exactly the total AGL contribution listed due to rounding. All values in eV/atom.

formula	PBE			LDA			SCAN		
	AGL-TVC	AGL-ZPC	AGL-TC	AGL-TVC	AGL-ZPC	AGL-TC	AGL-TVC	AGL-ZPC	AGL-TC
Ag_2CrO_4	−0.003	0.002	−0.006	−0.001	0.007	−0.008	−0.002	0.006	−0.008
Al_2SiO_5 (kya.)	0.019	0.041	−0.022	0.022	0.045	−0.023	0.023	0.046	−0.023
Al_2SiO_5 (and.)	0.016	0.036	−0.020	0.019	0.040	−0.021	0.019	0.041	−0.022
$BaAl_2O_4$	0	0.010	−0.010	0.001	0.013	−0.012	0.001	0.013	−0.012
$BaMoO_4$	−0.003	0.006	−0.009	−0.001	0.009	−0.011	−0.002	0.008	−0.010
$BaTiO_3$	0	0.013	−0.013	0.002	0.017	−0.015	0.002	0.017	−0.015
$BaZrO_3$	−0.001	0.011	−0.012	0.001	0.014	−0.014	0	0.014	−0.013
$BeAl_2O_4$	0.017	0.037	−0.020	0.020	0.041	−0.021	0.021	0.042	−0.021
Be_2SiO_4	0.016	0.033	−0.018	0.018	0.036	−0.018	0.019	0.037	−0.019
$CaAl_4O_7$	0.010	0.027	−0.017	0.012	0.031	−0.019	0.012	0.031	−0.019
$CaMoO_4$	0.004	0.019	−0.015	0.007	0.024	−0.017	0.006	0.023	−0.016
Ca_3SiO_5	0.006	0.022	−0.017	0.008	0.028	−0.019	0.008	0.026	−0.018
$CaSiO_3$ (wol.)	0.009	0.027	−0.018	0.011	0.031	−0.020	0.010	0.030	−0.019
$CaSiO_3$ (ps-wol.)	0.008	0.026	−0.018	0.011	0.030	−0.019	0.010	0.029	−0.019
$CaTiO_3$	0.010	0.029	−0.019	0.013	0.034	−0.021	0.012	0.033	−0.021
$Ca_2V_2O_7$	0.006	0.022	−0.016	0.009	0.027	−0.018	0.008	0.026	−0.018
CaV_2O_6	0.005	0.020	−0.015	0.009	0.026	−0.017	0.007	0.024	−0.017
$CaWO_4$	0.001	0.013	−0.012	0.003	0.017	−0.014	0.002	0.016	−0.014
$CaZrO_3$	0.005	0.022	−0.017	0.007	0.026	−0.018	0.007	0.025	−0.018
$CdAl_2O_4$	0.005	0.020	−0.015	0.007	0.023	−0.016	0.007	0.023	−0.016
$CdGa_2O_4$	0.002	0.015	−0.014	0.003	0.018	−0.015	0.003	0.019	−0.015
$CdTiO_3$	0.002	0.016	−0.013	0.004	0.019	−0.015	0.004	0.019	−0.015
$CoFe_2O_4$	0.001	0.009	−0.008	0.011	0.026	−0.016	0.005	0.017	−0.012
$CoTiO_3$	0.008	0.024	−0.016	0.013	0.031	−0.018	0.011	0.028	−0.017
$CuFeO_2$	0.005	0.017	−0.012	0.006	0.019	−0.013	0.003	0.014	−0.011
$FeAl_2O_4$	0.010	0.027	−0.017	0.013	0.030	−0.017	0.014	0.032	−0.019
$FeMoO_4$	0.006	0.021	−0.015	0.009	0.025	−0.016	0.006	0.021	−0.015
$FeTiO_3$	0.008	0.024	−0.016	0.014	0.033	−0.019	0.012	0.029	−0.018
$LiAlO_2$	0.018	0.039	−0.021	0.021	0.044	−0.022	0.022	0.045	−0.023
Li_3AsO_4	0.007	0.022	−0.015	0.009	0.026	−0.017	0.010	0.027	−0.017
Li_2SiO_3	0.016	0.036	−0.020	0.019	0.040	−0.021	0.019	0.040	−0.021

TABLE XI. (*continued*)

formula	PBE			LDA			SCAN		
	AGL-TVC	AGL-ZPC	AGL-TC	AGL-TVC	AGL-ZPC	AGL-TC	AGL-TVC	AGL-ZPC	AGL-TC
Li_2TiO_3	0.015	0.035	−0.020	0.019	0.040	−0.021	0.019	0.040	−0.021
Li_2ZrO_3	0.009	0.025	−0.017	0.011	0.029	−0.018	0.011	0.029	−0.018
$MgAl_2O_4$	0.015	0.036	−0.020	0.018	0.039	−0.021	0.018	0.040	−0.022
$MgCr_2O_4$	0.006	0.020	−0.014	0.009	0.025	−0.016	0.008	0.023	−0.015
$MgMoO_4$	0.004	0.018	−0.014	0.007	0.022	−0.015	0.006	0.021	−0.015
Mg_2SiO_4	0.013	0.032	−0.019	0.015	0.036	−0.021	0.015	0.036	−0.021
$MgSiO_3$	0.015	0.035	−0.020	0.018	0.039	−0.021	0.018	0.039	−0.021
$MgTiO_3$	0.012	0.032	−0.019	0.015	0.036	−0.021	0.015	0.036	−0.021
$MgTi_2O_5$	0.011	0.029	−0.018	0.014	0.034	−0.020	0.014	0.034	−0.020
MgV_2O_6	0.007	0.023	−0.016	0.014	0.033	−0.020	0.013	0.032	−0.019
$Mg_2V_2O_7$	0.008	0.025	−0.017	0.011	0.029	−0.018	0.011	0.029	−0.018
$MgWO_4$	0.003	0.017	−0.014	0.005	0.020	−0.015	0.005	0.020	−0.015
$MnTiO_3$	0.005	0.019	−0.013	0.009	0.024	−0.015	0.008	0.023	−0.015
$NaCrO_2$	0.005	0.021	−0.016	0.009	0.027	−0.018	0.008	0.025	−0.017
Na_2CrO_4	0.004	0.019	−0.016	0.007	0.024	−0.018	0.007	0.024	−0.018
$NaFeO_2$	0.002	0.013	−0.011	0.002	0.015	−0.012	0.003	0.017	−0.014
Na_2MoO_4	0.004	0.019	−0.015	0.006	0.023	−0.017	0.006	0.023	−0.017
Na_4SiO_4	0.006	0.023	−0.018	0.008	0.027	−0.019	0.008	0.028	−0.020
Na_2SiO_3	0.008	0.026	−0.019	0.010	0.030	−0.020	0.010	0.030	−0.020
$Na_2Ti_3O_7$	0.009	0.027	−0.019	0.012	0.032	−0.020	0.012	0.032	−0.020
$NaVO_3$	0.005	0.020	−0.015	0.008	0.025	−0.017	0.007	0.025	−0.017
Na_2WO_4	0.001	0.013	−0.012	0.003	0.017	−0.014	0.003	0.017	−0.014
$NiAl_2O_4$	0.010	0.026	−0.016	0.013	0.030	−0.018	0.013	0.031	−0.018
$NiTiO_3$	0.008	0.023	−0.015	0.011	0.028	−0.017	0.010	0.027	−0.017
$NiWO_4$	0.002	0.013	−0.012	0.004	0.017	−0.013	0.004	0.017	−0.013
$PbMoO_4$	−0.004	0.002	−0.006	−0.003	0.005	−0.008	−0.003	0.005	−0.008
$PbTiO_3$	−0.003	0.004	−0.007	−0.001	0.009	−0.010	−0.001	0.008	−0.009
$PbWO_4$	−0.005	0.001	−0.006	−0.003	0.004	−0.007	−0.004	0.004	−0.007
$SrAl_2O_4$	0.003	0.017	−0.014	0.005	0.020	−0.015	0.005	0.020	−0.015
$SrHfO_3$	−0.001	0.011	−0.012	0	0.014	−0.013	0	0.013	−0.013
$SrMoO_4$	0	0.012	−0.012	0.002	0.016	−0.014	0.001	0.015	−0.014
$SrSiO_3$	0.001	0.014	−0.013	0.003	0.018	−0.015	0.003	0.017	−0.014
Sr_2TiO_4	0.001	0.015	−0.014	0.003	0.018	−0.015	0.003	0.018	−0.015
$SrTiO_3$	0.004	0.020	−0.016	0.006	0.024	−0.018	0.006	0.024	−0.018
$SrWO_4$	−0.002	0.008	−0.010	0	0.012	−0.012	0	0.011	−0.012
$ZnFe_2O_4$	−0.003	0	−0.004	0.009	0.025	−0.016	0.005	0.019	−0.014
Zn_2SiO_4	0.004	0.017	−0.013	0.006	0.020	−0.014	0.006	0.021	−0.015
Zn_2TiO_4	0.005	0.020	−0.015	0.007	0.023	−0.016	0.008	0.024	−0.016
$ZnWO_4$	0.002	0.015	−0.013	0.004	0.018	−0.014	0.004	0.018	−0.014
$ZrSiO_4$	0.011	0.029	−0.019	0.013	0.033	−0.020	0.013	0.033	−0.020

TABLE XII: **AGL contributions to the formation enthalpies for ternary halides.** Total vibrational (TVC), zero-point (ZPC) and thermal (TC) contributions to the calculated formation enthalpies obtained from AGL [12–16] for each functional for ternary halides. The sum of ZPC and TC might not match exactly the total AGL contribution listed due to rounding. All values in eV/atom.

formula	PBE			LDA			SCAN		
	AGL-TVC	AGL-ZPC	AGL-TC	AGL-TVC	AGL-ZPC	AGL-TC	AGL-TVC	AGL-ZPC	AGL-TC
KBF_4	0.005	0.013	−0.008	0.008	0.020	−0.012	0.007	0.018	−0.011
Li_3AlF_6	0.016	0.029	−0.013	0.019	0.034	−0.016	0.019	0.034	−0.015
Li_2BeF_4	0.009	0.018	−0.008	0.012	0.022	−0.010	0.011	0.022	−0.010
Na_3AlF_6	0.011	0.022	−0.011	0.013	0.026	−0.013	0.013	0.026	−0.013
$NaBF_4$	0.008	0.019	−0.010	0.011	0.025	−0.013	0.011	0.024	−0.013
Na_2SiF_6	0.015	0.028	−0.014	0.017	0.033	−0.016	0.017	0.033	−0.016
$NaAlCl_4$	0.010	0.009	0.001	0.012	0.015	−0.003	0.012	0.014	−0.002

TABLE XIII: **Formation energies and CCE corrections for binary oxides.** DFT formation energies (without vibrational contribution) and experimental room temperature formation enthalpies, corrections per bond $\delta H_{A-\mathrm{O}}^{A+\alpha}$, number of cation-oxygen bonds $N_{A-\mathrm{O}}$ per formula unit and oxidation states $+\alpha$ of the cation for binary oxides. Experimental values from Kubaschewski *et al.* [3], NIST-JANAF [1] and Barin [4]. Values in brackets denote cases in which the corrections are applied to calculate corrected values (see section II of the main text for details). The O-O bond correction for peroxides is obtained from Li_2O_2. The O-O bond correction for superoxides is derived from KO_2. The two values are listed in the table at the position of the respective compound. Energies and enthalpies in eV/atom; corrections in eV/bond.

formula	PBE	LDA	SCAN	Exp.	$\delta H_{A-\mathrm{O}}^{A+\alpha}$ PBE	$\delta H_{A-\mathrm{O}}^{A+\alpha}$ LDA	$\delta H_{A-\mathrm{O}}^{A+\alpha}$ SCAN	$N_{A-\mathrm{O}}$	$+\alpha$
Li_2O	−1.861	−2.107	−2.097	−2.066 [3]	0.0766	−0.0154	−0.0118	8	+1
Li_2O_2	−1.436	−1.718	−1.618	−1.643 [3]	−0.0930	−0.1160	0.2400	12	+1
BeO	−2.768	−3.142	−3.146	−3.158 [3]	0.1953	0.0083	0.0060	4	+2
Na_2O	−1.225	−1.455	−1.474	−1.444 [1]	0.0823	−0.0043	−0.0113	8	+1
Na_2O_2	−1.084	−1.354	−1.288	−1.329 [3]	(−1.307)	(−1.312)	(−1.314)	12	+1
NaO_2	−0.794	−1.016	−0.894	−0.901 [3]	(−0.776)	(−0.918)	(−0.855)	6	+1
MgO	−2.717	−3.110	−3.124	−3.118 [3]	0.1335	0.0025	−0.0023	6	+2
K_2O	−1.033	−1.325	−1.264	−1.255 [3]	0.0830	−0.0263	−0.0035	8	+1
K_2O_2	−1.071	−1.386	−1.254	−1.282 [3]	(−1.297)	(−1.278)	(−1.303)	12	+1
KO_2	−0.888	−1.160	−1.011	−0.983 [3]	−0.5450	−0.2690	−0.0490	10	+1
CaO	−2.973	−3.389	−3.357	−3.290 [3]	0.1057	−0.0332	−0.0222	6	+2
Rb_2O	−0.917	−1.228	−1.158	−1.171 [3]	0.0950	−0.0215	0.0049	8	+1
SrO	−2.744	−3.126	−3.115	−3.068 [3]	0.1082	−0.0192	−0.0155	6	+2
SrO_2	−1.898	−2.313	−2.174	−2.189 [3]	(−2.228)	(−2.210)	(−2.203)	10	+2
Cs_2O	−0.994	−1.309	−1.205	−1.195 [3]	0.1008	−0.0567	−0.0050	6	+1
CsO_2	−0.890	−1.168	−1.003	−0.989 [3]	(−1.045)	(−0.889)	(−0.970)	10	+1
BaO	−2.486	−2.811	−2.828	−2.841 [3]	0.1183	0.0098	0.0042	6	+2
BaO_2	−1.860	−2.250	−2.123	−2.191 [3]	(−2.223)	(−2.244)	(−2.217)	10	+2
B_2O_3	−2.406	−2.723	−2.696	−2.640 [3]	0.1952	−0.0693	−0.0472	6	+3
Al_2O_3	−3.025	−3.491	−3.503	−3.473 [3]	0.1869	−0.0073	−0.0124	12	+3
SiO_2 (α-qua.)	−2.810	−3.178	−3.175	−3.147 [3]	0.2530	−0.0233	−0.0208	4	+4
SiO_2 (α-crist.)	−2.817	−3.167	−3.167	−3.138 [3]	(−3.154)	(−3.136)	(−3.139)	4	+4
Ga_2O_3	−1.856	−2.244	−2.180	−2.258 [3]	0.2009	0.0068	0.0386	10	+3
GeO_2	−1.605	−2.075	−1.924	−2.004 [3]	0.1992	−0.0357	0.0397	6	+4
As_2O_5	−1.073	−1.453	−1.332	−1.362 [3]	0.2022	−0.0636	0.0212	10	+5
SeO_2	−0.703	−1.005	−0.874	−0.778 [3]	0.0750	−0.2277	−0.0963	3	+4
In_2O_3	−1.595	−1.959	−1.950	−1.919 [3]	0.1353	−0.0167	−0.0130	12	+3
SnO	−1.347	−1.609	−1.507	−1.481 [4]	0.0670	−0.0638	−0.0130	4	+2
SnO_2	−1.706	−2.099	−2.037	−2.007 [4]	0.1505	−0.0460	−0.0153	6	+4
Sb_2O_3	−1.340	−1.621	−1.508	−1.484 [3]	0.1207	−0.1135	−0.0198	6	+3
SbO_2	−1.385	−1.764	−1.627	−1.567 [3]	(−1.571)	(−1.556)	(−1.557)	5	+3, +5
Sb_2O_5	−1.259	−1.666	−1.537	−1.439 [4]	0.1052	−0.1323	−0.0573	12	+5
TeO_2	−1.033	−1.388	−1.235	−1.117 [4]	0.0630	−0.2033	−0.0885	4	+4
Tl_2O	−0.591	−0.711	−0.701	−0.578 [3]	−0.0065	−0.0665	−0.0612	6	+1
Tl_2O_3	−0.681	−1.034	−0.843	−0.809 [3]	0.0536	−0.0936	−0.0140	12	+3
PbO	−1.131	−1.355	−1.246	−1.137 [3]	0.0028	−0.1088	−0.0548	4	+2
Pb_3O_4	−1.056	−1.311	−1.182	−1.064 [3]	(−1.107)	(−1.111)	(−1.113)	12	+2, +4
PbO_2	−0.835	−1.198	−0.998	−0.948 [3]	0.0568	−0.1250	−0.0250	6	+4
Bi_2O_3	−1.235	−1.533	−1.254	−1.183 [3]	−0.02580	−0.1752	−0.0356	10	+3
Sc_2O_3	−3.567	−3.976	−4.017	−3.956 [3]	0.1618	−0.0083	−0.0257	12	+3
TiO	−2.541	−2.973	−2.876	−2.812 [3]	0.1131	−0.0667	−0.0265	4.8	+2
Ti_2O_3	−2.917	−3.358	−3.318	−3.153 [3]	0.0980	−0.0855	−0.0688	12	+3
Ti_3O_5	−2.975	−3.373	−3.375	−3.186 [3]	(−3.202)	(−3.172)	(−3.179)	18	+3, +4
TiO_2 (rut.)	−3.047	−3.454	−3.509	−3.261 [3]	0.1072	−0.0965	−0.1237	6	+4
TiO_2 (ana.)	−3.078	−3.464	−3.517	−3.243 [1]	(−3.293)	(−3.271)	(−3.270)	6	+4
VO	−1.446	−1.877	−1.767	−2.237 [3]	0.2637	0.1203	0.1568	6	+2
V_2O_3	−2.290	−2.685	−2.654	−2.526 [3]	0.0984	−0.0661	−0.0531	12	+3
VO_2	−2.373	−2.765	−2.773	−2.466 [3]	0.0467	−0.1497	−0.1537	6	+4
V_2O_5	−2.307	−2.598	−2.607	−2.295 [3]	−0.0082	−0.2118	−0.2179	10	+5
Cr_2O_3	−1.985	−2.243	−2.397	−2.352 [3]	0.1528	0.0454	−0.0189	12	+3
CrO_3	−1.653	−1.826	−1.802	−1.521 [3]	−0.1323	−0.3053	−0.2813	4	+6
MnO	−1.240	−1.185	−2.092	−1.994 [3]	0.2513	0.2700	−0.0325	6	+2
MnO_2	−1.680	−1.988	−2.116	−1.800 [3]	0.0600	−0.0943	−0.1582	6	+4
FeO	−0.881	−1.017	−1.353	−1.410 [1]	0.1763	0.1310	0.0188	6	+2

TABLE XIII. (*continued*)

formula	PBE	LDA	SCAN	Exp.	$\delta H_{A-\mathrm{O}}^{A+\alpha}$ PBE	$\delta H_{A-\mathrm{O}}^{A+\alpha}$ LDA	$\delta H_{A-\mathrm{O}}^{A+\alpha}$ SCAN	$N_{A-\mathrm{O}}$	$+\alpha$
Fe_2O_3	−1.315	−1.676	−1.864	−1.707 [3]	0.1633	0.0130	−0.0655	12	+3
CoO	−0.513	−0.734	−0.863	−1.232 [3]	0.2397	0.1662	0.1230	6	+2
NiO	−0.474	−0.776	−0.648	−1.242 [3]	0.2558	0.1552	0.1980	6	+2
Cu_2O	−0.415	−0.544	−0.505	−0.590 [1]	0.1310	0.0340	0.0635	4	+1
CuO	−0.606	−0.860	−0.795	−0.808 [1]	0.1015	−0.0258	0.0068	4	+2
ZnO	−1.446	−1.732	−1.726	−1.817 [3]	0.1853	0.0423	0.0455	4	+2
Y_2O_3	−3.623	−4.001	−4.065	−3.949 [3]	0.1358	−0.0219	−0.0483	12	+3
ZrO_2	−3.466	−3.897	−3.939	−3.791 [1]	0.1393	−0.0451	−0.0631	7	+4
NbO	−2.057	−2.428	−2.344	−2.175 [3]	0.0593	−0.1263	−0.0845	4	+2
MoO_2	−1.973	−2.400	−2.242	−2.031 [3]	0.0292	−0.1843	−0.1053	6	+4
MoO_3	−1.978	−2.272	−2.187	−1.931 [3]	−0.0470	−0.3410	−0.2558	4	+6
RuO_2	−1.063	−1.465	−1.277	−1.054 [3]	−0.0048	−0.2057	−0.1118	6	+4
Rh_2O_3	−0.703	−1.064	−0.877	−0.737 [3]	0.0141	−0.1363	−0.0583	12	+3
PdO	−0.483	−0.757	−0.647	−0.599 [3]	0.0578	−0.0793	−0.0245	4	+2
Ag_2O	−0.118	−0.179	−0.194	−0.107 [3]	−0.0083	−0.0540	−0.0653	4	+1
CdO	−1.026	−1.290	−1.323	−1.339 [3]	0.1042	0.0162	0.0053	6	+2
HfO_2	−3.577	−4.024	−4.017	−3.955 [4]	0.1617	−0.0296	−0.0269	7	+4
WO_2	−1.923	−2.354	−2.133	−2.037 [3]	0.0567	−0.1587	−0.0483	6	+4
WO_3	−2.176	−2.495	−2.388	−2.183 [3]	0.0050	−0.2078	−0.1362	6	+6
ReO_2	−1.372	−1.799	−1.509	−1.551 [4]	0.0897	−0.1242	0.0212	6	+4
ReO_3	−1.635	−1.982	−1.766	−1.526 [4]	−0.0727	−0.3040	−0.1597	6	+6
OsO_2	−0.894	−1.306	−1.015	−1.018 [3]	0.0617	−0.1443	0.0012	6	+4
OsO_4	−0.994	−1.119	−1.038	−0.816 [3]	−0.2225	−0.3793	−0.2773	4	+8
IrO_2	−0.798	−1.201	−0.802	−0.838 [4]	0.0202	−0.1813	0.0180	6	+4
HgO	−0.300	−0.535	−0.412	−0.470 [3]	0.1700	−0.0650	0.0580	2	+2

TABLE XIV: **Formation energies and CCE corrections for binary halides.** DFT formation energies (without vibrational contribution) and experimental room temperature formation enthalpies, corrections per bond $\delta H_{A-X}^{A+\alpha}$, number of cation-anion bonds N_{A-X} per formula unit and oxidation states $+\alpha$ of the cation for binary halides. Experimental values from Kubaschewski *et al.* [3] and NIST-JANAF [1]. Note that BF_3 and SiF_4 are gaseous molecular systems. Energies and enthalpies in eV/atom; corrections in eV/bond.

formula	PBE	LDA	SCAN	Exp.	$\delta H_{A-X}^{A+\alpha}$ PBE	$\delta H_{A-X}^{A+\alpha}$ LDA	$\delta H_{A-X}^{A+\alpha}$ SCAN	N_{A-X}	$+\alpha$
LiF	−2.972	−3.176	−3.356	−3.197 [1]	0.0748	0.0070	−0.0532	6	+1
NaF	−2.739	−2.914	−3.133	−2.982 [1]	0.0807	0.0225	−0.0503	6	+1
KF	−2.736	−2.928	−3.094	−2.946 [1]	0.0702	0.0060	−0.0490	6	+1
BeF_2	−3.280	−3.483	−3.721	−3.547 [3]	0.2008	0.0480	−0.1300	4	+2
BF_3(g)	−2.786	−2.850	−3.092	−2.943 [3]	0.2093	0.1247	−0.1987	3	+3
AlF_3	−3.560	−3.851	−4.118	−3.913 [3]	0.2353	0.0415	−0.1367	6	+3
SiF_4(g)	−3.121	−3.232	−3.494	−3.348 [3]	0.2833	0.1450	−0.1825	4	+4
NaCl	−1.840	−1.970	−2.086	−2.131 [3]	0.0972	0.0537	0.0152	6	+1
KCl	−1.988	−2.124	−2.220	−2.263 [3]	0.0913	0.0460	0.0142	6	+1
$CaCl_2$	−2.436	−2.611	−2.713	−2.747 [3]	0.1552	0.0680	0.0167	6	+2
$AlCl_3$	−1.551	−1.768	−1.770	−1.828 [3]	0.1845	0.0400	0.0388	6	+3

TABLE XV: **Uncorrected and CCE corrected formation energies for ternary oxides.** DFT formation energies (without vibrational contribution), coordination corrected values (using corrections from Table XIII) and experimental room temperature formation enthalpies, number of cation-oxygen bonds $N_{1/2-\mathrm{O}}$ per formula unit and oxidation states $+\alpha$ of the cations for ternary oxides. For the cation-oxygen bonds- and oxidation numbers, the first (second) number in the column refers to the first (second) element in the formula. Experimental values from Kubaschewski *et al.* [3], NIST-JANAF [1] and Barin [4]. Energies and enthalpies in eV/atom.

formula	PBE	LDA	SCAN	PBE CCE	LDA CCE	SCAN CCE	Exp.	$N_{1/2-\mathrm{O}}$	$+\alpha$
Ag_2CrO_4	−1.100	−1.284	−1.300	−1.013	−1.032	−1.046	−1.083 [4]	10, 4	+1, +6
Al_2SiO_5 (kya.)	−2.937	−3.388	−3.386	−3.343	−3.365	−3.357	−3.361 [1]	12, 4	+3, +4
Al_2SiO_5 (and.)	−2.956	−3.373	−3.383	−3.339	−3.351	−3.356	−3.358 [1]	11, 4	+3, +4
$BaAl_2O_4$	−3.064	−3.403	−3.483	−3.405	−3.405	−3.473	−3.441 [3]	7.5, 8	+2, +3
$BaMoO_4$	−2.613	−2.871	−2.874	−2.739	−2.657	−2.709	−2.674 [4]	8, 4	+2, +6

TABLE XV. (*continued*)

formula	PBE	LDA	SCAN	PBE CCE	LDA CCE	SCAN CCE	Exp.	$N_{1/2-O}$	$+\alpha$
$BaTiO_3$	−3.090	−3.528	−3.540	−3.503	−3.436	−3.402	−3.441 [4]	12, 6	+2, +4
$BaZrO_3$	−3.301	−3.697	−3.745	−3.752	−3.666	−3.679	−3.689 [4]	12, 6	+2, +4
$BeAl_2O_4$	−2.970	−3.405	−3.419	−3.402	−3.397	−3.401	−3.407 [3]	4, 12	+2, +3
Be_2SiO_4	−2.794	−3.179	−3.175	−3.162	−3.175	−3.170	−3.134 [1]	8, 4	+2, +4
$CaAl_4O_7$	−3.074	−3.425	−3.492	−3.367	−3.402	−3.466	−3.477 [4]	5, 16	+2, +3
$CaMoO_4$	−2.598	−2.922	−2.892	−2.707	−2.650	−2.692	−2.671 [3]	8, 4	+2, +6
Ca_3SiO_5	−3.007	−3.403	−3.388	−3.331	−3.327	−3.334	−3.373 [3]	18, 4	+2, +4
$CaSiO_3$ (wol.)	−3.047	−3.423	−3.421	−3.383	−3.363	−3.376	−3.389 [3]	$6.\overline{3}$, 4	+2, +4
$CaSiO_3$ (ps-wol.)	−3.026	−3.401	−3.404	−3.398	−3.330	−3.352	−3.375 [3]	8, 4	+2, +4
$CaTiO_3$	−3.173	−3.604	−3.621	−3.470	−3.435	−3.437	−3.442 [3]	8, 6	+2, +4
$Ca_2V_2O_7$	−2.810	−3.127	−3.160	−2.928	−2.914	−2.955	−2.905 [3]	13, 9	+2, +5
CaV_2O_6	−2.647	−2.926	−2.959	−2.708	−2.669	−2.702	−2.682 [3]	6, 10	+2, +5
$CaWO_4$	−2.662	−2.987	−2.960	−2.806	−2.804	−2.840	−2.842 [4]	8, 4	+2, +6
$CaZrO_3$	−3.335	−3.734	−3.766	−3.629	−3.640	−3.664	−3.662 [3]	6, 6	+2, +4
$CdAl_2O_4$	−2.443	−2.841	−2.846	−2.823	−2.838	−2.827	−2.838 [3]	4, 12	+2, +3
$CdGa_2O_4$	−1.646	−2.002	−1.953	−2.050	−2.023	−2.022	−2.007 [3]	4, 12	+2, +3
$CdTiO_3$	−2.291	−2.634	−2.683	−2.545	−2.537	−2.541	−2.551 [4]	6, 6	+2, +4
$CoFe_2O_4$	−1.144	−1.465	−1.593	−1.561	−1.582	−1.551	−1.612 [3]	4, 12	+2, +3
$CoTiO_3$	−2.097	−2.431	−2.499	−2.513	−2.515	−2.498	−2.503 [3]	6, 6	+2, +4
$CuFeO_2$	−0.925	−1.281	−1.325	−1.236	−1.318	−1.258	−1.329 [3]	2, 6	+1, +3
$FeAl_2O_4$	−2.411	−2.753	−2.843	−2.832	−2.815	−2.832	−2.954 [4]	4, 12	+2, +3
$FeMoO_4$	−1.643	−2.044	−2.065	−1.788	−1.948	−1.913	−1.831 [3]	6, 4	+2, +6
$FeTiO_3$	−2.238	−2.520	−2.707	−2.579	−2.561	−2.581	−2.565 [3]	6, 6	+2, +4
$LiAlO_2$	−2.738	−3.123	−3.132	−3.133	−3.088	−3.096	−3.080 [3]	6, 6	+1, +3
Li_3AsO_4	−1.946	−2.209	−2.198	−2.162	−2.154	−2.191	−2.205 [4]	12, 4	+1, +5
Li_2SiO_3	−2.561	−2.867	−2.866	−2.832	−2.831	−2.836	−2.848 [3]	8, 4	+1, +4
Li_2TiO_3	−2.668	−3.005	−3.025	−2.929	−2.878	−2.878	−2.884 [3]	12, 6	+1, +4
Li_2ZrO_3	−2.768	−3.088	−3.112	−3.061	−3.012	−3.025	−3.044 [3]	12, 6	+1, +4
$MgAl_2O_4$	−2.991	−3.411	−3.434	−3.388	−3.400	−3.411	−3.404 [1]	4, 12	+2, +3
$MgCr_2O_4$	−2.231	−2.468	−2.629	−2.569	−2.547	−2.595	−2.632 [3]	4, 12	+2, +3
$MgMoO_4$	−2.375	−2.640	−2.633	−2.477	−2.416	−2.460	−2.419 [3]	6, 4	+2, +6
Mg_2SiO_4	−2.838	−3.218	−3.230	−3.211	−3.209	−3.214	−3.223 [3]	12, 4	+2, +4
$MgSiO_3$	−2.826	−3.220	−3.222	−3.189	−3.205	−3.203	−3.210 [3]	6, 4	+2, +4
$MgTiO_3$	−2.983	−3.372	−3.413	−3.272	−3.259	−3.262	−3.260 [3]	6, 6	+2, +4
$MgTi_2O_5$	−3.029	−3.402	−3.451	−3.289	−3.259	−3.264	−3.251 [1]	6, 12	+2, +4
MgV_2O_6	−2.487	−2.796	−2.817	−2.566	−2.563	−2.573	−2.534 [3]	6, 10	+2, +5
$Mg_2V_2O_7$	−2.581	−2.878	−2.922	−2.721	−2.726	−2.761	−2.671 [3]	12, 8	+2, +5
$MgWO_4$	−2.450	−2.806	−2.756	−2.588	−2.601	−2.618	−2.621 [3]	6, 6	+2, +6
$MnTiO_3$	−2.447	−2.648	−3.052	−2.877	−2.856	−2.865	−2.817 [3]	6, 6	+2, +4
$NaCrO_2$	−1.905	−2.127	−2.296	−2.258	−2.188	−2.251	−2.271 [3]	6, 6	+1, +3
Na_2CrO_4	−1.979	−2.186	−2.215	−2.021	−2.005	−2.038	−1.987 [4]	10, 4	+1, +6
$NaFeO_2$	−1.554	−1.717	−1.944	−1.799	−1.726	−1.867	−1.809 [3]	4, 4	+1, +3
Na_2MoO_4	−2.123	−2.352	−2.364	−2.238	−2.149	−2.198	−2.175 [4]	12, 4	+1, +6
Na_4SiO_4	−2.098	−2.381	−2.406	−2.375	−2.362	−2.374	−2.420 [3]	18, 4	+1, +4
Na_2SiO_3	−2.369	−2.667	−2.687	−2.674	−2.644	−2.655	−2.700 [3]	10, 4	+1, +4
$Na_2Ti_3O_7$	−2.796	−3.128	−3.178	−3.016	−2.988	−2.993	−3.007 [3]	10, 17	+1, +4
$NaVO_3$	−2.350	−2.563	−2.626	−2.442	−2.389	−2.439	−2.379 [4]	6, 4	+1, +5
Na_2WO_4	−2.175	−2.399	−2.419	−2.319	−2.273	−2.322	−2.283 [3]	12, 4	+1, +6
$NiAl_2O_4$	−2.289	−2.654	−2.672	−2.755	−2.730	−2.764	−2.844 [3]	4, 12	+2, +3
$NiTiO_3$	−2.077	−2.408	−2.406	−2.513	−2.479	−2.495	−2.492 [3]	6, 6	+2, +4
$NiWO_4$	−1.661	−1.984	−1.889	−1.922	−1.931	−1.951	−1.950 [3]	6, 6	+2, +6
$PbMoO_4$	−1.888	−2.131	−2.063	−1.861	−1.759	−1.819	−1.819 [3]	8, 4	+2, +6
$PbTiO_3$	−2.346	−2.684	−2.654	−2.458	−2.413	−2.443	−2.476 [3]	8, 5	+2, +4
$PbWO_4$	−1.944	−2.184	−2.121	−1.950	−1.900	−1.957	−1.937 [3]	8, 4	+2, +6
$SrAl_2O_4$	−3.077	−3.424	−3.494	−3.383	−3.399	−3.466	−3.442 [4]	6, 8	+2, +3
$SrHfO_3$	−3.415	−3.827	−3.844	−3.782	−3.760	−3.787	−3.697 [3]	8, 6	+2, +4
$SrMoO_4$	−2.624	−2.920	−2.906	−2.737	−2.667	−2.715	−2.676 [3]	8, 4	+2, +6
$SrSiO_3$	−3.040	−3.405	−3.414	−3.415	−3.355	−3.372	−3.386 [3]	8, 4	+2, +4
Sr_2TiO_4	−3.075	−3.495	−3.508	−3.445	−3.363	−3.363	−3.387 [3]	18, 6	+2, +4
$SrTiO_3$	−3.168	−3.603	−3.628	−3.556	−3.441	−3.442	−3.463 [3]	12, 6	+2, +4
$SrWO_4$	−2.686	−2.981	−2.972	−2.833	−2.817	−2.861	−2.832 [4]	8, 4	+2, +6

TABLE XV. (*continued*)

formula	PBE	LDA	SCAN	PBE CCE	LDA CCE	SCAN CCE	Exp.	$N_{1/2-O}$	$+\alpha$
$ZnFe_2O_4$	−1.284	−1.678	−1.788	−1.670	−1.725	−1.702	−1.735 [4]	4, 12	+2, +3
Zn_2SiO_4	−2.057	−2.382	−2.376	−2.414	−2.417	−2.416	−2.433 [3]	8, 4	+2, +4
Zn_2TiO_4	−2.120	−2.465	−2.487	−2.476	−2.442	−2.446	−2.443 [3]	10, 6	+2, +4
$ZnWO_4$	−1.939	−2.286	−2.217	−2.129	−2.120	−2.127	−2.126 [3]	6, 6	+2, +6
$ZrSiO_4$	−3.156	−3.592	−3.600	−3.510	−3.517	−3.502	−3.496 [1]	8, 4	+4, +4

TABLE XVI: **Uncorrected and CCE corrected formation energies for ternary halides.** DFT formation energies (without vibrational contribution), coordination corrected values (using corrections from Table XIV) and experimental room temperature formation enthalpies, number of cation-anion bonds $N_{1/2-X}$ per formula unit and oxidation states $+\alpha$ of the cations for ternary halides. For the cation-oxygen bonds- and oxidation numbers, the first (second) number in the column refers to the first (second) element in the formula. Experimental values from Kubaschewski *et al.* [3] and NIST-JANAF [1]. Energies and enthalpies in eV/atom.

formula	PBE	LDA	SCAN	PBE CCE	LDA CCE	SCAN CCE	Exp.	$N_{1/2-X}$	$+\alpha$
KBF_4	−3.040	−3.243	−3.433	−3.297	−3.336	−3.219	−3.255 [3]	10, 4	+1, +3
Li_3AlF_6	−3.246	−3.462	−3.682	−3.487	−3.496	−3.529	−3.507 [1]	$13.\overline{3}$, 6	+1, +3
Li_2BeF_4	−3.145	−3.310	−3.524	−3.345	−3.346	−3.389	−3.365 [3]	8, 4	+1, +2
Na_3AlF_6	−3.090	−3.280	−3.520	−3.360	−3.341	−3.358	−3.433 [3]	16, 6	+1, +3
$NaBF_4$	−2.969	−3.162	−3.360	−3.216	−3.275	−3.161	−3.187 [3]	8, 4	+1, +3
Na_2SiF_6	−3.103	−3.333	−3.535	−3.399	−3.459	−3.346	−3.354 [3]	12, 6	+1, +4
$NaAlCl_4$	−1.707	−1.828	−1.916	−1.911	−1.899	−1.955	−1.973 [1]	5, 4	+1, +3

[1] M. W. Chase, *NIST-JANAF Thermochemical Tables* (American Chemical Society and American Institute of Physics for the National Institute of Standards and Technology, Woodbury, NY, 1998), 4th edn.

[2] V. Stevanović, S. Lany, X. Zhang, and A. Zunger, *Correcting density functional theory for accurate predictions of compound enthalpies of formation: Fitted elemental-phase reference energies*, Phys. Rev. B **85**, 115104 (2012).

[3] O. Kubaschewski, C. B. Alcock, and P. J. Spencer, *Materials Thermochemistry* (Pergamon Press, Oxford, UK, 1993), 6th edn.

[4] I. Barin, *Thermochemical Data of Pure Substances* (VCH, Weinheim, 1995), 3rd edn.

[5] D. D. Wagman, et al., *The NBS tables of chemical thermodynamic properties*, J. Phys. Chem. Ref. Data **11**, Supplement No. 2 (1982).

[6] L. Wang, T. Maxisch, and G. Ceder, *Oxidation energies of transition metal oxides within the GGA+U framework*, Phys. Rev. B **73**, 195107 (2006).

[7] S. Lany, *Semiconductor thermochemistry in density functional calculations*, Phys. Rev. B **78**, 245207 (2008).

[8] J. Sun, A. Ruzsinszky, and J. P. Perdew, *Strongly Constrained and Appropriately Normed Semilocal Density Functional*, Phys. Rev. Lett. **115**, 036402 (2015).

[9] Z.-h. Yang, M. R. Pederson, and J. P. Perdew, *Full self-consistency in the Fermi-orbital self-interaction correction*, Phys. Rev. A **95**, 052505 (2017).

[10] B. Hammer, L. B. Hansen, and J. K. Nørskov, *Improved adsorption energetics within density-functional theory using revised Perdew-Burke-Ernzerhof functionals*, Phys. Rev. B **59**, 7413–7421 (1999).

[11] D. Hicks, et al., *AFLOW-SYM: platform for the complete, automatic and self-consistent symmetry analysis of crystals*, Acta Crystallogr. Sect. A **74**, 184–203 (2018).

[12] M. A. Blanco, et al., *Thermodynamical properties of solids from microscopic theory: Applications to MgF_2 and Al_2O_3*, J. Mol. Struct.: Theochem **368**, 245–255 (1996).

[13] M. A. Blanco, E. Francisco, and V. Luaña, *GIBBS: isothermal-isobaric thermodynamics of solids from energy curves using a quasi-harmonic Debye model*, Comput. Phys. Commun. **158**, 57–72 (2004).

[14] C. Toher, et al., *High-throughput computational screening of thermal conductivity, Debye temperature, and Grüneisen parameter using a quasiharmonic Debye model*, Phys. Rev. B **90**, 174107 (2014).

[15] C. Toher, et al., *Combining the AFLOW GIBBS and elastic libraries to efficiently and robustly screen thermomechanical properties of solids*, Phys. Rev. Materials **1**, 015401 (2017).

[16] J.-P. Poirier, *Introduction to the Physics of the Earth's Interior* (Cambridge University Press, 2000), 2nd edn.